arXiv:cond-mat/9701079v1 [cond-mat.mes-hall] 10 Jan 1997

Spin Ensemble Density Functional Theory for Inhomogeneous Quantum Hall Systems.

M.I. Lubin, O.Heinonen, and M.D. Johnson
Department of Physics, University of Central Florida, Orlando, Florida 32816-2385

We have developed an ensemble density functional theory which includes spin degrees of freedom for nonuniform quantum Hall systems. We have applied this theory using a local-spin-density approximation to study the edge reconstruction of parabolically confined quantum dots. For a Zeeman splitting below a certain critical value, the edge of completely polarized maximum density droplet reconstructs into a spin-unpolarized structure. For larger Zeeman splittings, the edge remains polarized and develops an exchange hole.

I. INTRODUCTION

The recent development of nanofabrication technology has made it possible to manufacture semiconductor systems with reduced dimensionality and very high electron mobility. These technological advances have led to the discovery of such fascinating phenomena as the fractional and integer quantum Hall effects (QHE)[1]. These occur in a two-dimensional electron gas in a magnetic field $\mathbf{B} = B\hat{z}$ perpendicular to the electron system[2]. A quantum treatment of the motion of an infinite, homogeneous system shows that the kinetic energy takes discrete values $(n+1/2)\hbar\omega_c$, where n is the Landau level index ($n = 0, 1, 2, \ldots$) and $\omega_c = eB/m^\star c$ is the cyclotron frequency. Each Landau level contains $n_B = B/\Phi_0$ states per unit area, or one state for each magnetic flux quantum $\Phi_0 = hc/e$, giving rise to a macroscopic Landau level degeneracy. The ratio of the electron areal density $n(\mathbf{r})$ to n_B defines the filling factor $\nu(\mathbf{r}) = n(\mathbf{r})/n_B$. The filling factor also can be expressed as $\nu = 2\pi l_B^2 n$, where $l_B = \sqrt{\hbar c/eB}$ is the magnetic length.

The fractional quantum Hall effect can occur when electron-electron interactions dominate disorder. At certain filling factors of the form $\nu = p/q$, with p and q relative primes and q odd, electron-electron interactions cause the condensation of the electrons into highly correlated states. These states are incompressible with an energy gap separating the ground state from the bulk excited states. However, in a finite system, there must exist gapless excitations localized near the edges[3]. Thus, the low-energy physics of finite systems is dominated by the gapless edge modes. Therefore, in is necessary to be able to accurately model edges of FQHE systems in order to explain experiments. In a finite FQHE system with the potential confining the electrons varying slowly compared to l_B, the electronic structure at the edges may form a series of alternating compressible and incompressible regions with a step-like density profile[4,5]. In addition to standard transport measurements, there are now a variety of probes to directly study edge structures in inhomogeneous systems. Examples are capacitance spectroscopy of the quantum Hall edges[6], time-resolved measurements of edge magnetoplasmons[7], and surface acoustic waves techniques which are capable of resolving very small spatial inhomogeneities in the electron density[8]. Addition spectroscopy has also been used to study quantum dots with sizes of the order of 100 nm and with 10 to 100 electrons[9].

For an explanation of experimental studies it is highly desirable to have a computational approach which accurately treats systems with of the order of $1 - 10^3$ electrons, and which can include effects such as accurate confinements, spin degrees of freedom, and finite layer thickness. Exact numerical diagonalizations are limited to very small systems ($N \leq 10$)[10,11]. Semiclassical methods[4,5] do not accurately treat electron-electron interactions, and effective field theories[12] cannot give accurate quantitative information about many system properties. A method that can deal with larger number of electrons is the composite fermion theory in the Hartree approximation[13]. However, in this approach, the singular Chern-Simons gauge field is replaced by its smooth spatial average, and the composite fermion mass has to be put into the calculations by hand. Furthermore, interpretation of the results is sometimes difficult and ambiguous. On the other hand, density functional theory (DFT) is known as a general quantitative method to include exchange-correlation effects in inhomogeneous systems without any fitting parameters. In this paper we show that it can be used to give highly accurate results for quantum Hall systems. Preliminary results for spin polarized systems were reported earlier[14,15].

The DFT was originally formulated by Hohenberg and Kohn as a practical method for a description of the ground state properties of many-body systems[16] . The foundation of DFT is the Hohenberg-Kohn theorem, which states that the ground state density uniquely determines the Hamiltonian of a system. Furthermore, a variational principle states that the ground state density minimizes the energy of the system. We will use the constrained search formulation of Levy[17] for the Hohenberg-Kohn theorem and its associated variational principle. In this elegant approach the ground state energy E can be written as a functional of density

$$E[n] = F[n] + \int d\mathbf{r}\, n(\mathbf{r}) V_{\rm ext}(\mathbf{r}). \tag{1}$$

Here

$$F[n] = \inf_{\Psi \to n} \langle \Psi | \hat{T} + \hat{V}_{\rm ee} | \Psi \rangle, \tag{2}$$

with $\hat{T}$, $\hat{V}_{\rm ee}$, and $\hat{V}_{\rm ext}$ kinetic energy, electron-electron interactions, and external potential, respectively. The infimum is taken over all many-body states Ψ that yield a fixed density $n(\mathbf{r})$. $F[n]$ so defined is then a universal functional of the density $n(\mathbf{r})$. For a given external potential $V_{\rm ext}$, the true ground state density is the function $n(\mathbf{r})$ which minimizes $E[n]$ in Eq. (1).

The origins of the DFT are to be found in the statistical method developed by Thomas and Fermi[18]. They first realized the advantage of describing an inhomogeneous systems by using the density

$$n(\mathbf{r}) = \int d\mathbf{r}_2 \ldots \int d\mathbf{r}_N \mid \Psi(\mathbf{r}, \mathbf{r}_2, \ldots, \mathbf{r}_N) \mid^2, \tag{3}$$

an observable, rather than the unobservable complex wave function Ψ of Nd variables in d dimensions. Thomas-Fermi theory is a way to find an approximate $n(\mathbf{r})$. The theory is valid in the semi-classical limit and has a successful history of applications to many different problems[19]. But since Thomas-Fermi method neglects exchange-correlation effects and makes an approximation for the kinetic energy functional, it has some serious deficiences as well. For example, Thomas-Fermi theory cannot predict ferromagnetism. DFT remedies these problems by explicitly (and formally exactly) incorporating exchange-correlation effects as well as interaction parts of the kinetic energy functional into an exchange and correlation energy functional $E_{\rm xc}[n(\mathbf{r})]$, and by developing a useful computational scheme for including exchange-correlation effects[20]. This is done by introducing an auxiliary non-interacting system with a ground-state density $n_s(\mathbf{r})$, and by asserting that there exists an effective potential $V_s(\mathbf{r})$ for this system such that $n_s(\mathbf{r}) = n(\mathbf{r})$, with $n(\mathbf{r})$ the ground-state density of the real, interacting system. A system with this property is called v-representable. The density is then obtained from a simple Slater-determinant of the so-called Kohn-Sham (KS) orbitals $\psi_\alpha(\mathbf{r})$, $n_s(\mathbf{r}) = \sum_{\alpha=1}^{N} |\psi_\alpha(\mathbf{r})|^2$, where $\psi_\alpha(\mathbf{r})$ are obtained by self-consistently solving the KS equations[20]

$$h_{\rm eff}\psi_\alpha(\mathbf{r}) = [T + V_s(\mathbf{r})]\, \psi_\alpha(\mathbf{r}) = \varepsilon_\alpha \psi_\alpha(\mathbf{r}). \tag{4}$$

The self-consistency is achieved in practice by iteratively obtaining the eigenstates and occupying the N eigenstates with the lowest eigenvalues ε_α. The effective potential $V_s(\mathbf{r})$ can be derived from the Hohenberg-Kohn theorem and its associated variational principle. First, the functional $E[n]$ [Eq. (1)] can be decomposed as

$$E[n] = T_0[n] + \int d\mathbf{r} n(\mathbf{r}) \left[V_{\rm ext}(\mathbf{r}) + \frac{1}{2} V_{\rm H}(\mathbf{r}) \right] + E_{\rm xc}[n]. \tag{5}$$

Here T_0 is the kinetic energy of a non-interacting system with density n, $V_{\rm H}$ is the classical (Hartree) Coulomb potential

$$V_{\rm H}(\mathbf{r}) = \frac{e^2}{\epsilon_0} \int d\mathbf{r}' \frac{n(\mathbf{r}')}{|\mathbf{r} - \mathbf{r}'|}, \tag{6}$$

with ϵ_0 the static dielectric constant, and $E_{\rm xc}$ may be viewed as a definition of the exchange-correlation energy. The non-interacting kinetic energy T_0 is treated exactly in this approach, which removes many of the deficiencies of the Thomas-Fermi model. The variational principle applied to Eq. (5) yields

$$\frac{\delta E[n]}{\delta n(\mathbf{r})} = \frac{\delta T_0}{\delta n(\mathbf{r})} + V_{\rm ext}(\mathbf{r}) + V_{\rm H}(\mathbf{r}) + V_{\rm xc}(\mathbf{r}) = \mu, \tag{7}$$

where μ is the Lagrange multiplier associated with the requirement of constant particle number, and the exchange-correlation potential $V_{\rm xc}$ is formally defined as the functional derivative

$$V_{\rm xc}(\mathbf{r}) \equiv \frac{\delta E_{\rm xc}[n]}{\delta n(\mathbf{r})}. \tag{8}$$

Comparison of Eq. (7) with the corresponding relationship for a non-interacting system,

$$\frac{\delta E[n]}{\delta n(\mathbf{r})} = \frac{\delta T_0}{\delta n(\mathbf{r})} + V_s(\mathbf{r}) = \mu, \tag{9}$$

gives an expression for the effective potential

$$V_s(\mathbf{r}) = V_{\rm ext}(\mathbf{r}) + V_{\rm H}(\mathbf{r}) + V_{\rm xc}(\mathbf{r}). \tag{10}$$

In Eq. (5) all terms but the exchange-correlation energy $E_{\rm xc}$ can be evaluated exactly. In practical calculations, the local density approximation (LDA) is often used[20]. In this approximation, one writes

$$E_{\rm xc}^{\rm LDA} = \int d\mathbf{r}\, n(\mathbf{r}) \epsilon_{\rm xc}(n(\mathbf{r})), \tag{11}$$

where $\epsilon_{\rm xc}(n)$ is the exchange-correlation energy per particle of an infinite, homogeneous system of density n. The exchange-correlation potential [Eq. (8)] is then obtained as

$$V_{\rm xc}^{\rm LDA}(\mathbf{r}) = \left.\frac{d\left[n\epsilon_{\rm xc}(n)\right]}{dn}\right|_{n=n(r)}. \tag{12}$$

Above we ignored the electron spin – $n(\mathbf{r})$ was the total electron density, and the spin degree of freedom was neglected. The Hohenberg-Kohn theorem formally ensures that *every* property, including the spin density or polarization, can be obtained from the ground-state density. However, practical LDA calculations of systems with spontaneously broken symmetries, such as spin rotation symmetry, typically are much improved if the order parameter of the broken symmetry, *e.g.,* spin density or polarization, is explicitly included by construction. In particular, the broken symmetry may not otherwise be obtained accurately from the LDA. In GaAs samples, where most of QHE experiments have been done, the spin degree of freedom is important, and may lead to inhomogeneous spin densities. This is because the effective Zeeman energy $g^*\mu_B B$ is quite small compared to the cyclotron energy $\hbar\omega_c$, $g^*\mu_B B/\hbar\omega_c \approx 0.02$, due to the small effective mass $m^* = 0.068 m_e$ and a reduced Landé g-factor $|g^*| = 0.44$. This means that in a uniform noninteracting system, two highly degenerate Zeeman levels with the same Landau level index n are almost degenerate in energy. Since the dielectric constant for GaAs $\epsilon_0 \approx 13$, the cyclotron energy $\hbar\omega_c$ and Coulomb energy $e^2/(\epsilon_0 l_B)$ are of the same order of magnitude for magnetic fields of the strength of a few Tesla ($\frac{\hbar\omega_c}{e^2/(\epsilon_0 l_B)} \approx 0.4\sqrt{B[\mathrm{T}]}$). Using the Coulomb energy as the unit of energy, the dimensionless parameter characterizing Zeeman coupling can then be defined as

$$\tilde{g} \equiv \frac{g^*\mu_B B}{e^2/(\epsilon_0 l_B)}. \tag{13}$$

The small value of $\tilde{g}$ (typically about 0.02) makes the existence of partly polarized states energetically possible[21,22] even at $\nu < 1$. Therefore, it is necessary to include the spin degree of freedom in any quantitative theoretical approach to QHE systems. A reasonable first step is to generalize the DFT to include the spin polarization[23,24]. An exact treatment of the spins, in general, requires[23] the replacement of the charge density $n(\mathbf{r})$ by the single-particle density matrix $\rho_{\sigma\sigma'}(\mathbf{r}) = \langle 0|\hat{\psi}^+_\sigma(\mathbf{r})\hat{\psi}_{\sigma'}(\mathbf{r})|0\rangle$. Here, $\hat{\psi}^+_\sigma(\mathbf{r})$ and $\hat{\psi}_\sigma(\mathbf{r})$ are the usual field operators corresponding to the annihilation and creation of an electron with spin σ at $\mathbf{r}$, and $|0\rangle$ is the ground state of the system. With a constant magnetic field applied in the z-direction, the $\hat{z}$ component of the total spin angular momentum is a constant of the motion and it is convenient to assume that the magnetization density only has a $\hat{z}$ component. Under this assumption, the single-particle density matrix can be taken to be diagonal, $\rho_{\sigma\sigma'}(\mathbf{r}) = \rho_{\sigma\sigma'}(\mathbf{r})\delta_{\sigma\sigma'}$. In this case the constrained search procedure of Eqs. (1) and (2) is modified to[25]

$$E[n_\uparrow, n_\downarrow] = F[n_\uparrow, n_\downarrow] + \int d\mathbf{r}\, n(\mathbf{r}) V_{\rm ext}(\mathbf{r}), \tag{14}$$

where $F[n_\uparrow, n_\downarrow] = \inf_{\Psi\to n}\langle\Psi|\hat{T} + \hat{E}_{\rm Z} + \hat{V}_{\rm ee}|\Psi\rangle$ and $\hat{E}_{\rm Z}$ is the Zeeman energy with Ψ yielding fixed densities $n_\sigma(\mathbf{r})$. The local spin-density approximation (LSDA) is then given by

$$E_{\rm xc}^{\rm LSDA}[n_\uparrow, n_\downarrow] = \int d\mathbf{r}\, n(\mathbf{r}) \epsilon_{\rm xc}[n_\uparrow(\mathbf{r}), n_\downarrow(\mathbf{r})], \tag{15}$$

where $\epsilon_{\rm xc}[n_\uparrow, n_\downarrow]$ is the exchange-correlation energy per particle in a homogeneous system with up- and down- spin densities $n_\uparrow$ and $n_\downarrow$, respectively. In spite of the LSDA being justified only in the limit of small spatial variations of the electron density, this approximation has been surprisingly successful in describing the properties of inhomogeneous

atomic, molecular and solid-state systems[26]. This scheme correctly predicted, for example, ferromagnetism in Fe, Co and Ni among the transition metals[26]. Moreover, the self-interaction-corrected LSDA was successfully applied to some strongly correlated systems such as the transition-metal oxides and a Hubbard model representing a CuO_2 layer in the cuprate superconductors[27].

In the original Kohn-Sham formulation [Eqs. (1) and (2)], the ground state was assumed to be nondegenerate and the ground state density $n(\mathbf{r})$ assumed to be pure-state v-representable. This means that $n(\mathbf{r})$ can be be expressed in terms of a single Slater determinant of KS orbitals $\psi_\alpha(\mathbf{r})$ obeying an effective single-particle Schrödinger equation [Eq. (4)]. However, there are systems which are known not to be v-representable in this sense. One class of such systems was considered independently by Levy[28] and Lieb[29]. Consider a system with q independent N-particle degenerate ground states $|\Psi_1\rangle, \ldots, |\Psi_q\rangle$. Then construct the density matrix

$$\hat{D} = \sum_{i=1}^{q} d_i |\Psi_i\rangle\langle\Psi_i| \tag{16}$$

with $d_i = d_i^* \geq 0$, $\sum_{i=1}^{q} d_i = 1$. This yields the density

$$n(\mathbf{r}) = \mathrm{Tr}\{\hat{D}\hat{n}(\mathbf{r})\} = \sum_{i=1}^{q} d_i n_i(\mathbf{r}), \tag{17}$$

where $n_i(\mathbf{r}) = \langle\Psi_i|\hat{n}(\mathbf{r})|\Psi_i\rangle$ (spin degrees of freedom are neglected for simplicity). As was proven by Levy and Lieb, if $q > 2$ the density $n(\mathbf{r})$ cannot be represented by a single ground state in DFT, *i.e.,* it cannot be obtained by a single Slater determinant of the N lowest energy KS orbitals. However, there exists a generalization of Hohenberg-Kohn theorem which provides a one-to-one correspondence between a ground state density $n(\mathbf{r})$ and the Hamiltonian even for system with a ground state density which can be of the form of Eq. (17). By extending the functional $F[n]$ in Eq. (2) to

$$F_{\mathrm{E}}[n] = \inf_{\hat{D}\to n} \mathrm{Tr}\{\hat{D}(\hat{T} + \hat{V_{\mathrm{ee}}})\}, \tag{18}$$

with the infimum taken over all $\hat{D}$ yielding a fixed density $n(\mathbf{r})$, there is then a generalized variational principle which states that $F_{\mathrm{E}}[n]$ is minimized by the ground state density, which can now be represented by an ensemble of wave functions, even if it cannot be represented by a single Slater determinant. This generalization is called *ensemble* density functional theory. As we shall see below, fractional QHE systems are not v-representable, so an ensemble DFT has to be used.

In Sec. II we review our ensemble DFT scheme. The essential features of our ensemble DFT approach will be illustrated in Sec. III by applying it to spin-polarized quantum Hall dot. Sec. IV then describes the spin-unpolarized edge reconstruction of $\nu = 1$ quantum Hall dot. The phase diagram for the spin textured edge reconstruction of the maximum density droplet will be presented there. Finally, conclusions are given in Sec. V.

II. PRACTICAL ALGORITHM FOR ENSEMBLE DENSITY FUNCTIONAL THEORY

In practical ensemble DFT calculations one introduces as in the KS scheme an auxiliary non-interacting system which provides the basis for the density matrix and has a ground state density identical to the interacting system at hand. By using the variational principle, one then arrives at a set of equations analogous[30] to the KS equations Eq. (4). However, the density for N electrons is now given by

$$n(\mathbf{r}) = \sum_{\alpha} f_\alpha |\psi_\alpha(\mathbf{r})|^2, \quad \sum_{\alpha} f_\alpha = N, \tag{19}$$

with the occupation numbers f_α in the interval $0 \leq f_\alpha \leq 1$. One obtains fractional occupancies f_α only when the corresponding KS eigenvalues ε_α are degenerate and equal to the Fermy energy ε_F. (If $\varepsilon_\alpha < \varepsilon_F$, then $f_\alpha = 1$.) Let us show briefly why applying DFT to the FQHE inevitably requires ensemble DFT. We consider an infinite, homogeneous fractional QHE system at a filling factor of $\nu = 1/3$, and assume that we have the *exact* exchange-correlation potential V_{xc} for this system. We then construct a set of determinantal N-particle wavefunctions $\{\Psi_i\}$ made up from the KS orbitals ψ_α obtained by solving the KS equation using the exact exchange-correlation potential. Label each member Ψ_i of this set by the set of numbers $\{\theta_{i\alpha}\}$ identifying the KS orbitals used to construct Ψ_i [$\theta_{i\alpha} = (0)1$ for (un)occupied orbitals, and $\sum_\alpha \theta_{i\alpha} = N$]. Because the KS orbitals are orthogonal, a state Ψ_i has density[31]

$$n_i(\mathbf{r}) = \sum_\alpha \theta_{i\alpha} |\psi_\alpha(\mathbf{r})|^2. \tag{20}$$

Construct three states Ψ_i, $i = 1, 2, 3$, with occupancies $\{\theta_{i\alpha}\} = \{100100\ldots\}, \{010010\ldots\}, \{001001\ldots\}$. The occupied KS orbitals are all degenerate lowest Landau level states (since the system is homogeneous), so the three Ψ_i are degenerate. Then construct a density matrix of the form of Eq. (16) with $d_1 = d_2 = d_3 = 1/3$. The resulting density $n(\mathbf{r})$ (Eq. 17) is constant: $n(\mathbf{r}) = \frac{1}{3}\frac{1}{2\pi l_B^2}$, corresponding to a uniform system with $\nu = 1/3$. Now we can appeal to the Levy-Lieb theorem[28,29]: since the $\nu = 1/3$ ground state density can be constructed as in Eqs. (16) and (17) with $q > 2$ degenerate states Ψ_i this density is therefore *not* pure state v-representable, and ensemble DFT must be used.

In inhomogeneous FQHE systems, not all KS orbitals are degenerate, but some are. By a simple extension of the argument in the paragraph above, such systems too are not pure state v-representable, and ensemble DFT must be used. For inhomogeneous systems one finds M orbitals with $\varepsilon_\alpha < \varepsilon_F$ and D degenerate orbitals with $\varepsilon_\alpha = \varepsilon_F$. One constructs determinantal wavefunctions Ψ_i in which all M low-energy orbitals are occupied; the Ψ_i differ by which $N - M$ of the D degenerate orbitals are occupied. Using Eq. (17) and the density of determinantal wavefunctions given in Eq. (20), the total density for the ensemble represented by $\hat{D}$ can be calculated as

$$n(\mathbf{r}) = \sum_\alpha \sum_{i=1}^{q} d_i \theta_{i\alpha} |\psi_\alpha(\mathbf{r})|^2. \tag{21}$$

Comparing the result with Eq.(19), one can see how the fractional occupational numbers f_α of the degenerate KS orbitals follow from the weights d_i in the expansion of density matrix $\hat{D}$:

$$f_\alpha = \sum_{i=1}^{q} d_i \theta_{i\alpha}. \tag{22}$$

As we mentioned in Sec. I, for the density defined by Eq. (21), a generalization of Hohenberg-Kohn theorem exists and an extended variational principle [Eq. (18)] can be used. However, a procedure to compute the fractional occupancies f_α has not existed[32], and one major advance in our work is that we have found a simple way to generate the occupancies, at least for the FQHE[14,15]. Applying ensemble DFT to the FQHE, we have found that fractionally-occupied KS orbitals are indeed degenerate at the Fermi energy, consistent with our demonstration above that the FQHE is in general not pure-state v-representable. We will review this scheme here.

In our algorithm, we start with a set of input occupancies and single-particle orbitals and iterate the system $N_{\rm eq}$ times using the KS scheme. The number $N_{\rm eq}$ is chosen large enough (about 20-40 in practical calculations) that the density is close to the final density after $N_{\rm eq}$ iterations. If the density of the system could be represented by a single Slater determinant of the KS orbitals, we would now essentially be done. However, in an "ensemble v-representable" (but not pure state v-representable) system there are many degenerate or near-degenerate KS orbitals at the Fermi energy, and small fluctuations in the density between iterations cause the KS scheme to occupy a different subset of these orbitals each iteration. This corresponds to constructing different Slater determinants Ψ_j each iteration. In other words, when the KS orbitals are degenerate at the Fermi energy there is an ambiguity in how to occupy these degenerate orbitals. Nevertheless, by associating the number of the iteration j with the particular Fock state Ψ_j represented by the occupation numbers $\theta_{j\alpha}$, one can accumulate the running average occupancies after each iteration

$$f_{\alpha,N_{\rm it}} = \frac{1}{N_{\rm it} - N_{\rm eq}} \sum_{j=N_{\rm eq}+1}^{N_{\rm it}} \theta_{j\alpha}, \tag{23}$$

where $N_{\rm it}$ is the number of iterations. This is clearly of the form of Eq. (22) with the weights d_i given by the relative frequency of the corresponding Slater determinant during $N_{\rm it} - N_{\rm eq}$ iterations. To achieve a self-consistent solution, the system of KS equations is then iterated using average occupancies $f_{\alpha,N_{\rm it}}$ instead of $\theta_{j\alpha}$, with the density after $N_{\rm it}$ iterations calculated as

$$n_{N_{\rm it}}(\mathbf{r}) = \sum_\alpha f_{\alpha,N_{\rm it}} |\psi_\alpha(\mathbf{r})|^2. \tag{24}$$

This density is used to calculate the new effective potential $V_s(\mathbf{r})$ according Eq.(10), and by solving the resulting KS equations a new set of occupancies $\theta_{j\alpha}$ is obtained, which can be again used to update averages $f_{\alpha,N_{it}}$. When a self-consistent solution is obtained this highly nonlinear map should give the same input and output densities after one iteration. To prove formally that this scheme with the running average occupancies converges self-consistently to

the physical density is by no means a trivial problem. However, we have numerically verified for FQHE systems that a finite-temperature version of our scheme converges to a thermal ensemble at finite temperatures down to temperatures of the order of $10^{-4}\hbar\omega_c/k_B$[15]. We have also performed Monte Carlo simulations about the ensemble obtained by our scheme. In these simulations, we used a Metropolis algorithm to randomly change the occupation numbers about our converged solution, keeping the chemical potential fixed. The free energy of the new set of occupation numbers was calculated self-consistently. The results were that to within numerical accuracy our scheme gives the lowest free energy. We have also checked our ensemble DFT against small system numerical diagonalizations with very good results (see Sec. III).

This algorithm has made ensemble DFT a practical calculation tool, and it may be possible to apply it to strongly correlated systems other than the QHE, for example inhomogeneous Mott insulators, provided there are accurate approximations for the ground state energies of homogeneous systems available.

III. SPIN-POLARIZED QUANTUM DOT IN A FQHE REGIME

In order to illustrate the essential features of our ensemble DFT scheme, we first neglect the spin degree of freedom and consider a spin-polarized quantum dot in the FQHE regime. Typical quantum dots contain about 10-100 electrons, so the quantum dot can be used as a model system in order to demonstrate the usefulness of the DFT in the study of large inhomogeneous electron systems. Moreover, quantum dots are believed to have highly correlated ground states in strong magnetic fields[33]. Hence, these systems can be used to show how well these strong correlation effects are represented by LDA compared to exact diagonalization studies[10,11]. There have been some attempts to use density functional theory to model such systems. Ferconi and Vignale[34] performed current-spin DFT studies of quantum dots in the integer QHE regime with a small number of electrons. In their calculations, the energy gaps due to correlation effects were not included, and the spin-dependence of the exchange-correlation energy was taken to be that of an electron gas in the $B \to 0$ limit. Their results for a spin-polarized three-electron system are in good agreement with results from exact diagonalizations. However, their approach cannot be extended to include fractionally occupied states or the complicated spin dependence of the exchange-correlation energy in the strong magnetic field region.

Electron-electron interactions in the ground state of quantum dots have been studied experimentally, for example by measuring the tunneling conductance through a Coulomb island[9,35]. The dots used experimentally can very accurately be modeled as parabolic[9], i.e., the Coulomb islands are confined by a parabolic potential $V_{ext} = m^*\Omega^2 r^2/2$, where m^* is the effective mass of an electron, Ω characterizes the strength of confining potential and r is the distance from the center of the dot. We chose this potential for our model system.

Due to the circular symmetry we can label the KS orbitals $\psi_\alpha(\mathbf{r})$ by Landau level index $n \geq 0$, and by angular momentum label $m \geq -n$ ($\alpha \equiv \{m,n\}$) and expand $\psi_\alpha(\mathbf{r})$ in the eigenstates $|mn\rangle$ of the single-particle Hamiltonian $\hat{T}_0 = (-i\hbar\nabla + \frac{e}{c}\mathbf{A})^2/2m^*$ as

$$\psi_{mn}(\mathbf{r}) = e^{im\phi}\varphi_{mn}(r) = \sum_{n'} C_{mnn'}\langle \mathbf{r}|mn'\rangle. \tag{25}$$

We can then solve self-consistently the KS equations $h_{\rm eff}\varphi_{mn} = \varepsilon_{mn}\varphi_{mn}$ for the radial parts φ_{mn} of KS orbitals for each value of the angular momentum m separately. The orthonormal basis $\langle \mathbf{r}|mn\rangle$ can be written in the cylindrical gauge $\mathbf{A} = \frac{1}{2}B(x,-y,0)$ in terms of the associated Laguerre polynomials[36] L_n^m

$$\langle \mathbf{r}|mn\rangle = \frac{1}{\sqrt{2\pi l_B^2}}\left(\frac{n!}{(n+m)!}\right)^{1/2}\left(\frac{r}{\sqrt{2}l_B}\right)^m L_n^m\left(\frac{r^2}{2l_B^2}\right)e^{im\phi - r^2/4l_B^2}. \tag{26}$$

These are centered on circles of radii $r_{mn} \approx \sqrt{2(m+n)}l_B$ with Gaussian fall-offs for $r \ll r_{mn}$ and $r \gg r_{mn}$. We write the density $n(\mathbf{r})$ in dimensionless form as a nonuniform filling factor $\nu(\mathbf{r}) = 2\pi l_B^2 n(\mathbf{r})$,

$$\nu = 2\pi l_B^2 \sum_{mn} f_{mn}|\psi_{mn}|^2 = \sum_{mnn'n''} f_{mn}C_{mnn'}C_{mnn''}\langle mn'|mn''\rangle. \tag{27}$$

This is used to calculate the effective potential $V_s(r)$ in the KS equations. In the lowest Landau level these expressions simplify (for example, the filling factor becomes just $\nu(r) = e^{-x}\sum_m f_{m0}\frac{x^m}{m!}$ with $x = r^2/4l_B^2$). However, we have used the four lowest Landau levels ($n = 0,\ldots,3$) and kept the general expressions, since as we mentioned in Sec. I, the cyclotron energy $\hbar\omega_c$ and Coulomb energy $e^2/(\epsilon_0 l_B)$ are of the same order of magnitude for typical experimental situation, so there can be appreciable Landau-level mixing. The solution of the KS equations in the basis $|mn\rangle$ reduces to iteratively obtaining the eigenstates with the lowest energies of the following block-diagonal Hamiltonian matrix

$$h_{\mathrm{eff},mn'n} = \hbar\omega_c(n+\frac{1}{2}) + \langle mn'|\hat{V}_s|mn\rangle, \tag{28}$$

where the effective potential $V_s(r) = V_{\mathrm{ext}}(r) + V_{\mathrm{H}}(r) + V_{\mathrm{xc}}(r)$ is defined by Eq.(10). We chose a confining potential of strength $\hbar\Omega = 1.6$ meV corresponding to that of McEuen *et al.*[9]. The Hartree potential for a circularly symmetric quantum dot is given by

$$V_{\mathrm{H}}(r) = \frac{e^2}{\epsilon_0 l_B}\int_0^{2\pi} d\phi \int dr' \frac{r'n(r')}{\sqrt{r^2+r'^2-2rr'\cos\phi+\delta z^2}}, \tag{29}$$

where δz is a finite thickness of the 2D electron liquid. The interaction of the 2D electrons with a gate can also be easily incorporated into the Hartree potential. Although the typical value of δz for a real experimental situation is about 10 nm, in our simulations we took $\delta z \to 0$ in order to compare our results with other theoretical works.

We have used the LDA to obtain the exchange-correlation potential V_{xc}. In this approximation, we first need the exchange-correlation energy per particle in a homogeneous system ϵ_{xc} which we chose as

$$\epsilon_{\mathrm{xc}}(\nu) = \epsilon_{\mathrm{xc}}^{\mathrm{LWM}}(\nu) + \epsilon_{\mathrm{xc}}^{\mathrm{C}}(\nu). \tag{30}$$

The first term is a smooth interpolation formula of Levesque *et al.*,[37]

$$\begin{aligned}\epsilon_{\mathrm{xc}}^{\mathrm{LWM}}(\nu) &= \int_0^\infty dr\ r\left(\frac{e^2}{r\epsilon_0 l_B}\right)[g_\nu(r)-1] \\ &\simeq -0.782133\sqrt{\nu}\left(1-0.211\nu^{0.74}+0.012\nu^{1.7}\right)(e^2/\epsilon_0 l_B)\end{aligned} \tag{31}$$

for the ground-state energy obtained by evaluating the pair correlation functions $g_\nu(r)$ at certain fillings $\nu < \frac{1}{2}$ for about 256 particles using very accurate Monte Carlo methods. The second term in Eq. (30), $\epsilon_{\mathrm{xc}}^{\mathrm{C}}(\nu)$, contains the cusps in the ground state energy which cause the FQHE. The discontinuity in the slope of $\epsilon_{\mathrm{xc}}^{\mathrm{C}}(\nu)$ near certain "magic" filling factors $\nu^\star = p/q$ is related to the chemical potential gap $\Delta\mu = q(|\Delta_p| + |\Delta_h|)$. Here $\Delta_{p,h}$ are the quasiparticle (hole) creation energies[38] at $\nu = \nu^\star$. In our calculations, we restrict ourselves to include only the cusps at $\nu = 1/3, 2/5, 3/5$ and $\nu = 2/3$, which are the strongest fractions. (See Appendix A for a detailed description of our expression for $\epsilon_{\mathrm{xc}}^{\mathrm{C}}$.) Substituting Eq. (30) into Eq. (12) we can find the exchange-correlation potential as a function of filling factor $V_{\mathrm{xc}}(\nu)$ for a spin-polarized system. This potential is depicted in Fig. (4) as $V_{\mathrm{xc},\uparrow}(\nu, \xi = 1)$ (the generalized spin DFT approach will be discussed later in Sec. IV).

The discontinuities in $V_{\mathrm{xc}}(\nu)$ in the LDA give rise to a numerical instability. The reason is that an arbitrarily small fluctuation in charge density close to an FQHE fraction gives rise to a finite change in energy that leads to serious convergence problems. To overcome this, we made the compressibility of the system finite, but very small, corresponding to a finite, but very large, curvature instead of a point-like cusp in ϵ_{xc} at the FQHE fractions. This was accomplished by allowing the discontinuity in chemical potential to occur over an interval in filling factor δ of magnitude 10^{-3}. This corresponds to a sound velocity of about 10^6 m/s in the electron gas, which is three orders of magnitude larger than the Fermi velocity of a 2D electron gas at densities typical for the FQHE. In general, the finite compressibility does not lead to any spurious physical effects so long as the energy of density fluctuations on a size of the order of the systems size is larger than any other relevant energy in the problem. The only noticeable effect is that incompressible plateaus, at which the density would be perfectly constant were the compressibility zero, have density fluctuations on a scale of δ.

We have used our ensemble DFT-LDA scheme to study the edge reconstruction of a 40-electron quantum dot as a function of magnetic field strength. For a certain range of magnetic field (typically about 2 – 3 T), it is known[40] that such a dot forms a so-called maximum density droplet. The maximum density droplet is spin-polarized with a filling factor which is unity in the bulk and falls off rapidly to zero at $r_0 \approx \sqrt{2N}\ell_B$. It is the most compact droplet (minimum angular momentum) that can be formed of spin-polarized electrons in the lowest Landau level. Increasing the magnetic field increases the importance of electron repulsion compared to confinement. At some higher magnetic field B, the edge of maximum density droplet is reconstructed, forming an exchange hole, because it becomes energetically favorable to spread out the electron density while still taking advantage of short-ranged attractive exchange interaction[40,41].

For a slowly varying confining potential, alternating compressible and incompressible strips in density may be formed[4,5] between $\nu = 1$ and $\nu = 0$ regions, with the density of the incompressible strips fixed at the density of an FQHE fraction, $\nu = p/q$. The widths of the incompressible strips are determined by the energy gaps at the fractions p/q, while the widths of the compressible strips are determined by electrostatics. These compressible and incompressible strips at the edge of an FQHE system were studied in an extended Thomas-Fermi approximation at

low but finite temperatures by Ferconi, Geller, and Vignale[43] for infinite Hall bars. Their results for the widths of the incompressible and compressible strips were in good agreement with the predictions by the semiclassical theories[4,5]. In the extended Thomas-Fermi approximation, the kinetic energy was treated as a local functional, as in the standard Thomas-Fermi approximation, while the exchange-correlation energy was included in a LDA. This extended Thomas-Fermi approximation is presumably valid in the limit of very slowly varying confining potential and large numbers of electrons. In contrast, our ensemble DFT approach (Sec. II) treats the kinetic energy exactly, and does not have any limitations on the number of the electrons. Furthermore our calculations can be done at very low or zero temperature.

Figure 1 depicts some of our results for a 40-electron droplet using our ensemble density functional approach. In these calculations, we chose a parabolic confinement of strength $\hbar\Omega = 1.6$ meV, and $\epsilon_0 = 12.4$, appropriate for GaAs, and $T = 0$. For values of the magnetic less than about 2.5 T, the droplet forms a maximum density droplet. At $B \approx 2.8$ T, an exchange-hole forms. This value of magnetic field compares very well with values obtained from Hartree-Fock calculations. For example, using $\epsilon_0 = 12.4$ and $\hbar\Omega = 1.6$ meV, we obtain from the work of MacDonald, Yang, and Johnson[40] a value of 2.52 T, while the value from the work of de Chamon and Wen[41] is 2.84 T. As the magnetic field is increased further, the effective confinement softens, and the droplet undergoes several reconstructions in which compressible and incompressible strips are formed. Figure 1 shows one example of incompressible strips at $\nu = 2/3$ and $\nu = 3/5$ for a magnetic field of 4.1 T. In our calculations, the incompressible strips form at filling factors where $V_{\rm xc}$ has a discontinuity. Traversing across an incompressible strip, the effective single-particle potential $(V_{\rm ext} + V_{\rm H} + V_{\rm xc})$ is constant – as $V_{\rm ext} + V_{\rm H}$ varies, $V_{\rm xc}$ varies across its discontinuity exactly to screen the change in $V_{\rm ext} + V_{\rm H}$. Thus, the width of the incompressible strips is determined by the distance over which $V_{\rm ext} + V_{\rm H}$ varies by an amount equal to a discontinuity in $V_{\rm xc}$, in agreement with the argument of Chklovskii, Shklovskii, and Glazman[5]. The widths of the compressible strips are determined by electrostatics plus the smooth parts of the exchange-correlation potential.

In order to compare our results with exact diagonalization studies of quantum Hall dots by Yang, MacDonald and Johnson[10] we have calculated the expectation value of the total angular momentum $\langle M \rangle = \sum_{mn} m f_{mn}$ as a function of the magnetic field strength B for $N = 6$ spin-polarized electrons in the lowest Landau level and a confining potential of $\hbar\Omega = 2.0$ meV. The results are shown in Fig. 2 for two different versions of the exchange-correlation energy $\varepsilon_{\rm xc}$. The diamonds ($\diamond$) were generated using the Levesque-Weiss-MacDonald exchange-correlation energy[37], while the plusses ($+$) were generated using an exchange-correlation energy due to Fano and Ortolani[42]. This latter is constructed not only to give the right behavior for $\nu < 1/2$, but both the value of $\varepsilon_{\rm xc}$ at $\nu = 1/2$ and particle-hole symmetry of the lowest Landau level are included to give a good interpolation formula on the entire interval $0 \leq \nu \leq 1$ for electrons in the lowest Landau level. Both exchange-correlation energies give clear plateaus or plateau-like structures in angular momentum *vs.* magnetic field. However, the Levesque-Weiss-MacDonald is a rather poor approximation near $\nu = 1$ (a region for which it was not constructed), and furthermore overestimates the magnitude of the exchange-correlation potential at about $\nu = 1/2$. As a consequence, the initial maximum density droplet instability is smeared out and starts at a too low value of magnetic field, and the formation of a 1/3 droplet (as is evidenced by studies of the density profile) occurs at a too high value of magnetic field. Also, the values of the angular momentum at the plateau-like regions tend to be too low. For example, the formation of the 1/3-droplet occurs at $M \approx 40$, while the exact value is $M = 45$. In contrast, the results obtained using Fano-Ortolani exchange-correlation energy tend to be very accurate. For example, the maximum density droplet instability occurs at $B \approx 2.8$ T in our calculations, compared to $B = 2.75$ T in the numerical diagonalizations, and the 1/3 droplet formation occurs at $B \approx 5.3$ T in our calculations, compared to $B = 5.29$ T in the numerical diagonalizations (see Fig. 3). In addition, the plateau-like regions are more developed and flatter in angular momentum. Still, though, the ensemble DFT tends to underestimate the angular momentum at the plateaus. We want to emphasize here that we have not used any adjusting parameters in our calculations. Furthermore, the ensemble DFT is not constructed so as to give only integer angular momentum. Finally, only the energy gaps at $\nu = 1/3$ and $\nu = 2/5$, along with their particle-hole conjugates at $\nu = 2/3$ and $\nu = 3/5$ were included, while the numerical diagonalizations used the full Coulomb interaction. Therefore, perfect agreement between our ensemble DFT results and the numerical diagonalizations cannot be expected. We also did these calculations at a finite temperatute of 100 mK ($k_B T/e^2/(\epsilon_0 l_B) \sim 1 \times 10^{-3}$), which improves the convergence of these small particle systems. In view of all this, the agreement between our ensemble DFT results and the numerical diagonalizations of Yang, MacDonald and Johnson[10] must be considered remarkable. We are presently working on extending the Fano-Ortolani interpolation to include $\nu \geq 1$ and several Landau levels.

IV. SPIN TEXTURED EDGE RECONSTRUCTION OF THE MAXIMUM DENSITY DROPLET.

The edge reconstruction of $\nu = 1$ maximum density droplet outlined in Sec. III suggests that $\nu = 1$ is much simpler to study than the fractional quantum Hall filling factors due to the absence of a cusp in $\epsilon_{\rm xc}(\nu)$ at $\nu = 1$. Therefore, one might expect that $\nu = 1$ is a Fermi liquid in the sense that the elementary excitations are well described by single-

particle excitations and only renormalized by the interactions. However, recent experiments on high mobility GaAs quantum wells[44] have provided evidence for the existence of topological charge-spin textures, so-called 'skyrmions', near $\nu = 1$. These are non-trivial many-body excitations due to electron-electron interactions first predicted to be the low-energy excitations near $\nu = 1$ by Sondhi et al.[45], with the energies about half of those of single-particle spin-flip excitations. The fact that skyrmions are the low-energy excitations near $\nu = 1$ (and also possibly near $\nu = 1/3$) raises the possibility of spin-textured edge reconstruction of the maximum density droplet. Therefore, inclusion of the spin degree of freedom may be essential in the study of inhomogeneous systems. Indeed, Hartree-Fock and effective field theoretical calculations have shown that for a soft confining potential, the edge of an infinite Hall bar at $\nu = 1$ becomes unstable to spin-textured reconstruction for weak Zeeman coupling, while stronger Zeeman coupling yields a spin-polarized reconstruction[46].

Motivated by these ideas, we have generalized our ensemble DFT approach to include spin degrees of freedom within the LSDA [Eq. (15)]. We have applied this generalization to parabolic maximum density droplets to study the edge reconstruction as a function of confinement strength (magnetic field) and Zeeman coupling. We find that as the Zeeman coupling is decreased, the edge becomes unstable to spin-textured reconstruction at a strength of the Zeeman coupling consistent with that found by Karlhede *et al.*[46] This provides further evidence for the importance of spin degrees of freedom in inhomogeneous systems and demonstrates the usefulness of our LSDA ensemble density functional approach.

For a parabolic dot, the variational principle applied to the KS functional [Eq. (14)] yields two sets of KS equations for spin up and spin down electrons

$$\left(T + V_{\mathrm{s},\sigma}(r,B)\right)\varphi_{mn,\sigma}(r) = \varepsilon_{mn,\sigma}\varphi_{mn,\sigma}(r), \tag{32}$$

where

$$V_{\mathrm{s},\sigma}(r,B) = \sigma g^{\star}\mu_0 B + V_{\mathrm{ext}}(r) + V_{\mathrm{H}}(r) + V_{\mathrm{xc},\sigma}(r,B) \tag{33}$$

is an effective potential for the auxiliary non-interacting system. In the LSDA the exchange-correlation potentials are

$$V_{\mathrm{xc},\sigma}(r,B) = \left.\frac{\partial}{\partial n_\sigma}\left(n\epsilon_{\mathrm{xc}}[n_\uparrow, n_\downarrow, B]\right)\right|_{n_\sigma = n_\sigma(r)}. \tag{34}$$

The parametric dependence on the magnetic field B can be incorporated by using spin filling factors $\nu_\sigma = 2\pi l_B^2 n_\sigma$ as variables instead of spin densities n_σ. To make connection with the spin-polarized case we first transform the spin filling factors ν_σ to total filling factor ν and spin polarization ξ:

$$\begin{aligned} \nu &= \nu_\uparrow + \nu_\downarrow \\ \xi &= (\nu_\uparrow - \nu_\downarrow)/(\nu_\uparrow + \nu_\downarrow). \end{aligned} \tag{35}$$

The exchange-correlation potentials (Eq.(34)) then become

$$\begin{aligned} V_{\mathrm{xc},\uparrow} &= \frac{\partial}{\partial\nu}\left(\nu\epsilon_{\mathrm{xc}}\right) + (1-\xi)\frac{\partial}{\partial\xi}\epsilon_{\mathrm{xc}}\ , \\ V_{\mathrm{xc},\downarrow} &= \frac{\partial}{\partial\nu}\left(\nu\epsilon_{\mathrm{xc}}\right) - (1+\xi)\frac{\partial}{\partial\xi}\epsilon_{\mathrm{xc}}\ , \end{aligned} \tag{36}$$

where the exchange-correlation energy per particle in a homogeneous system with a filling factor ν and polarization ξ, *i.e.,* $\epsilon_{\mathrm{xc}} \equiv \epsilon_{\mathrm{xc}}(\nu,\xi)$, has to be approximated.

We already have given the expression for the exchange-correlation energy per particle for the spin-polarized electron gas $\epsilon_{\mathrm{xc}}(\nu, \xi = 1)$ [Eq. (30)]. The question is then how to obtain a reasonable interpolation formula for ϵ_{xc} between spin-polarized ($\xi = 1$) and spin-unpolarized ($\xi = 0$) 2D electron liquids for a fixed ν in a strong magnetic field. We have constructed a reasonable first approximation, as we now explain.

In what follows x(c) as a subscript denotes exchange (correlation) respectively. We decompose the exchange-correlation energy E_{xc} into exchange E_{x} and correlation E_{c} energies. Since the exchange interaction only acts between parallel spins, we have

$$E_{\mathrm{x}}[\nu_\uparrow, \nu_\downarrow] = \frac{1}{2}E_{\mathrm{x}}[\nu_\uparrow, \nu_\uparrow] + \frac{1}{2}E_{\mathrm{x}}[\nu_\downarrow, \nu_\downarrow]. \tag{37}$$

Moreover, it follows from dimensional analysis that the exchange energy must scale as density (filling factor) to the 3/2 power in a 2D electron gas. Following Oliver and Perdew[47], we can then write:

$$E_{\rm x} \sim \int d^2r \left[\nu_\uparrow^{3/2}(r) + \nu_\downarrow^{3/2}(r)\right]. \tag{38}$$

We also have from Eqs. (35) $\nu_\uparrow = \frac{1}{2}\nu(1-\xi)$, $\nu_\downarrow = \frac{1}{2}\nu(1+\xi)$. Equation (38) can then be rewritten as

$$E_{\rm x} \sim \int d^2r\ \nu^{3/2}\left[(1+\xi)^{3/2} + (1-\xi)^{3/2})\right]. \tag{39}$$

Since in the local density approximation for the exchange energy $E_{\rm x} = \int d^2r\nu\epsilon_{\rm x}(\nu,\xi)$ we are then led to the form

$$\begin{aligned}\epsilon_{\rm x}(\nu,\xi) &= \epsilon_{\rm x}(\nu,\xi=1) + (\epsilon_{\rm x}(\nu,\xi=0) - \epsilon_{\rm x}(\nu,\xi=1))f(\xi)\\ &\equiv \epsilon_{\rm x}(\nu,\xi=1) + \Delta\epsilon_{\rm x}(\nu,\xi),\end{aligned} \tag{40}$$

where the function

$$f(\xi) = \frac{(1+\xi)^{3/2} + (1-\xi)^{3/2} - 2\sqrt{2}}{2-2\sqrt{2}} \tag{41}$$

is an interpolation function between the two extreme cases $\xi = 0$ and $\xi = 1$ with $f(0) = 1$ and $f(1) = 0$. Although the analogous simple closed form for the correlation energy $\epsilon_{\rm c}(\nu,\xi)$ is not available, it can be always be written as $\epsilon_{\rm c}(\nu,\xi) = \epsilon_{\rm c}(\nu,\xi=1) + \Delta\epsilon_{\rm c}(\nu,\xi)$. So, as a first approximation we will use the form of Eq. (40) for the smooth part of the correlation energy $\epsilon_{\rm c}$, too (leaving the cusps aside for the moment), with the *same* interpolation function $f(\xi)$, as was suggested first by von Barth and Hedin[23]. Denoting the smooth part of the exchange-correlation energy per particle by $\epsilon_{\rm xc}^{\rm s}$ we can then write

$$\begin{aligned}\epsilon_{\rm xc}^{\rm s}(\nu,\xi) &= \epsilon_{\rm xc}^{\rm s}(\nu,\xi=1) + \left[\epsilon_{\rm xc}^{\rm s}(\nu,\xi=0) - \epsilon_{\rm xc}^{\rm s}(\nu,\xi=1)\right] f(\xi)\\ &\equiv \epsilon_{\rm xc}^{\rm s}(\nu,\xi=1) + \delta\epsilon_{\rm xc}(\nu) f(\xi).\end{aligned} \tag{42}$$

So far, we have constructed a function $\epsilon_{\rm xc}^{\rm s}(\nu,\xi)$ which gives a smooth interpolation for the exchange-correlation energy for any value of ν and ξ. What is left is to add the cusps to this function. We already have a good approximation for these at $\xi = 1$. We now need to extend this approximation to arbitrary values of ξ. Very little is known about the cusps, *i.e.,* the energy gaps, for arbitrary polarizations. It is known that there *is* a gap for un-polarized systems at fillings $\nu = 2/5$, $\nu = 3/5$, and $\nu = 2/3$. The gap, and thus the cusps, occur at very special 'magic' configurations at which the system can take advantage of a particularly low correlation energy. Therefore, it seems plausible that for a given value of ν, say $\nu = 2/5$, there cannot be an energy gap for any value of ξ between 0 and 1. In order to incorporate this assumption into a usable approximation, we interpolate our cusp energy constructed for polarized systems, $\epsilon_{\rm xc}^{\rm C}(\nu)$, to arbitrary polarizations by multiplying it by a function $g(\xi)$ which is unity at $\xi = 0$ and $\xi = 1$ with zero derivative at these points, vanishes away from these values of polarization, and is symmetric about $\xi = 1/2$. All together, then, we have

$$\epsilon_{\rm xc}(\nu,\xi) = \epsilon_{\rm xc}^{\rm LWM}(\nu) + \delta\epsilon_{\rm xc}(\nu)f(\xi) + \epsilon_{\rm xc}^{\rm C}(\nu)g(\xi). \tag{43}$$

Specifically, we chose

$$g(\xi) = \left[4\xi^2 - 1\right]^2 \left[27 - \xi^2\left(40 - 16\xi^2\right)\right]/27, \tag{44}$$

which is the only polynomial in ξ satisfying the above constraints. Near $\nu = 1$ (where there is no cusp in the total exchange-correlation energy), the sign of the function $\delta\epsilon_{\rm xc}(\nu)$ will then determine the spin polarized (ferromagnetic) or spin unpolarized (paramagnetic) ground state of the infinite electron liquid (neglecting the Zeeman splitting). Indeed, substitution of Eq. (43) into Eq. (36) gives

$$\Delta V_{\rm xc} \equiv V_{{\rm xc},\uparrow} - V_{{\rm xc},\downarrow} = 2\frac{\partial}{\partial\xi}\epsilon_{\rm xc} = 2\delta\epsilon_{\rm xc}(\nu)f'(\xi) + 2\epsilon_{\rm xc}^{\rm C}(\nu)g'(\xi). \tag{45}$$

The last term in this expression may be ignored near $\nu = 1$. We would thus expect a spin-polarized ground state if $\delta\epsilon_{\rm xc}(\nu) > 0$ because $f'(\xi) < 0$ for all $0 \le \xi \le 1$ so in this case the inequality $V_{{\rm xc},\uparrow} < V_{{\rm xc},\downarrow}$ holds. Otherwise we would expect a spin unpolarized state. Since a von Barth-Hedin type approximation has been applied before only to the 3D electron gas in zero magnetic field, it is natural to ask how faithful this approximation is[49] to data obtained from the numerical diagonalization studies[22,48] outlined in Table I. First, reversed spins are in fact possible in the ground state of quantum Hall liquids. It is known from numerical studies[50] that the electron gas is completely polarized only

at filling factors $\nu = 1, \frac{1}{3}, \frac{1}{5}$. Secondly, there are some partially polarized ground states that cannot be realized in the approximation used here because the function $f(\xi)$ is monotonic. If the partially polarized states were realized by this function it would have a minimum at some fractional ξ. However, the simple model Eq. (42) allows us to capture the essential physics of the spin unpolarized edge reconstruction of the quantum dot as it will be shown on the example below.

In order to obtain the function $\delta\epsilon_{\rm xc}(\nu)$ in Eq. (43) we start by calculating the energy differences between spin polarized and unpolarized states for fractions listed in Table I. The value for the ground state energy of a $\nu = 1$ unpolarized system is not available, but a reasonable approximation is to take $\epsilon_{\rm xc}(\nu = 1, \xi = 0) = \epsilon_{\rm xc}(\nu = 1/2, \xi = 1) = -0.469\ (e^2/\epsilon_0 l_B)$, implying that the spin-up and spin-down components are uncorrelated. The ground state energy of a $\nu = 1$ polarized system $\epsilon_{\rm xc}(\nu = 1, \xi = 1) = -0.6265\ (e^2/\epsilon_0 l_B)$. Therefore we have $\delta\epsilon_{\rm xc}(\nu = 1) = 0.1575\ (e^2/\epsilon_0 l_B)$. The last quantity is close to the energy required for a exchange-enhanced single spin flip, $\sqrt{\pi/8}(e^2/\epsilon_0 l_B)$, at this filling[51]. To complete the numerical parameterization of exchange-correlation functional, we then perform a spline fit to obtain the function $\delta\epsilon_{\rm xc}(\nu)$. We have plotted the exchange-correlation potentials $V_{{\rm xc},\sigma}$ as a function of a filling factor ν at $\xi = 1$ and $\xi = 0$ in Fig. 4. We see that at $\xi = 1$ the difference between exchange-correlation potentials for spin up and spin down electrons $\Delta V_{\rm xc}$ [Eq. (45)] is changing sign from negative to positive while the filling factor ν is decreasing from $\nu = 1$ to $\nu = 2/3$. Ignoring the Zeeman splitting and the cusps, the ground state of an infinite electron liquid would change from spin polarized to spin unpolarized. To estimate the possibility of having a spin unpolarized state above filling 2/3 with the inclusion of the Zeeman splitting, we have to compare the dimensionless Zeeman energy $\tilde{g}$ [Eq. (13)] with the difference $\Delta V_{\rm xc}$ [Eq. (45)] at this filling $\Delta V_{\rm xc}(\nu = 2/3, \xi = 1) \approx 0.05(e^2/\epsilon_0 l_B)$. This value is larger then the Zeeman splitting for GaAs $\tilde{g} \approx 0.02$. Therefore, the ground state of a GaAs based homogeneous system is a spin unpolarized state at and just above filling factor 2/3. In an inhomogeneous system, in addition to exchange-correlation potential and Zeeman energy, there are also the Hartree interaction of the 2D electrons and the external potential which confines them. Hence, even in von Barth and Hedin type approximation, it is possible to have not only polarized and unpolarized states, but also a partially polarized state in inhomogeneous system such a quantum dot.

We have investigated the spin density of a quantum dot using our LSDA ensemble DFT. The results, choosing the same parameters as in Sec. III, are shown in Fig. 5. We find that the electron liquid is indeed partially polarized at the quantum dot edge provided the Zeeman energy is small enough (Fig. 5). For Zeeman energies below a certain critical value, $\tilde{g} < \tilde{g}_c$, the maximum density droplet is reconstructed with the increasing of the magnetic field by forming an unpolarized (in general partially polarized) state. However, as $\tilde{g}$ increases above the critical value, $\tilde{g} > \tilde{g}_c$, the polarized reconstruction described in Sec. III takes place. We can plot the phase diagram of the edge reconstruction of the quantum dot in the $(\tilde{g}, \tilde{\gamma})$ plane (Fig. 6), where the dimensionless parameter $\tilde{\gamma} = m^*\Omega^2 l_B^2/(e^2/\epsilon_0 l_B)$ characterizes the 'softness' of the edge. The phase boundaries separate the maximum density droplet, spin polarized and unpolarized instabilities. The value of $\tilde{g}_c \approx 0.055$ separating the spin-polarized and spin-structured instabilities is in good agreement with the value $\tilde{g}_c^{\rm YMJ} \approx 0.03$ found from numerical diagonalization of parabolic dots by Yang, MacDonald and Johnson[10]. A phase diagram analogous to ours was obtained in the work by A. Karlhede *et al.*[46]. Their value of the critical Zeeman splitting $\tilde{g}_c^{\rm KKLS} = 0.169$ obtained by Hartree-Fock calculations is about 3 times larger then $\tilde{g}_c \approx 0.055$ from our phase diagram. We speculate that the difference is due to the the fact that correlations were ignored in their Hartree-Fock calculation, and to the different geometry they used – an infinite Hall bar.

V. SUMMARY AND CONCLUSIONS

We have developed a spin ensemble density functional approach to strongly correlated systems and used it to study inhomogeneous quantum Hall systems in the integer and fractional Hall regimes. For spin-polarized systems, our approach gives results in excellent agreement with numerical diagonalizations, Hartree-Fock and semi-classical calculations. Note that while all of these latter approaches have limited regions of applicability, such as small systems, systems near $\nu = 1$, or the semi-classical limit, we have here demonstrated that our ensemble density functional approach spans all these regions, which makes it a useful approach to general inhomogeneous quantum Hall systems.

We have generalized the ensemble DFT to include spin degrees of freedom within a simple local spin density approximation, and applied this generalization to a quantum dot. Our results show that for small, but physical, Zeeman energies, $\tilde{g} < \tilde{g}_c$, the maximum density droplet is unstable with respect to spin-textured edge reconstructions as the magnetic field increased. At larger Zeeman splittings, $\tilde{g} > \tilde{g}_c$, the maximum density droplet is unstable with respect to spin-polarized edge reconstructions. Our value of $\tilde{g}_c$ is in good agreement with that obtained from numerical diagonalization studies[10]. Hartree-Fock calculations for an infinite Hall bar by A. Karlhede *et al.*[46] give a phase diagram qualitatively analogous to ours. However, Hartree-Fock calculations are limited to $\nu \approx 1$, while our

ensemble DFT is in principle applicable to general fractional quantum Hall systems, e.g. droplets at $\nu = \frac{1}{3}$. The accuracy of our approach depends on obtaining good estimates of the exchange-correlation energy as a function of both electron density and spin polarization for homogeneous fractional quantum Hall systems. Work is currently in progress to obtain such estimates. Finally, the spin ensemble DFT used here cannot be used to study spin-charge textures (skyrmions), in which the spin polarization rotates smoothly in space. Work is currently under way to generalize our spin DFT to include such charge-spin textures.

The authors would like to thank M. Ferconi, M. Geller and G. Vignale for helpful discussions and for sharing their results prior to publication, K. Burke and E.K.U Gross for useful comments about the DFT, M. Levy for a discussion about Ref. 28, and J.M. Kinaret for help with the LSDA. O.H. would like to thank Chalmers Institute of Technology, where part of the work was done. This work was supported by the NSF through grants DMR93-01433 and DMR96-32141.

APPENDIX

We will construct the cusp-part of the exchange-correlation energy, $\epsilon_{\rm xc}^{\rm C}(\nu)$ for a spin-polarized system by first considering $\nu < 1/2$, and then use electron-hole symmetry to obtain the form for $1/2 < \nu < 1$. Finally, for $\nu > 1$ we assume $\epsilon_{\rm xc}^{\rm C}(\nu) = \epsilon_{\rm xc}^{\rm C}(1-\nu)$.

For spin-polarized systems in the lowest Landau level, we write $\epsilon_{\rm xc}(\nu) = \epsilon'_{\rm xc}(\nu) + \epsilon_{\rm xc}^{\rm C}(\nu)$, where $\epsilon'_{\rm xc}(\nu)$ is given by a smooth interpolation, such as the Levesque-Weiss-MacDonald formula[37] (although this one does not obey strict particle-hole symmetry in the lowest Landau level), or the Fano-Ortolani formula[42]. Particle-hole symmetry yields for the total exchange-correlation energy

$$\nu\left[\epsilon_{\rm xc}(\nu) - \epsilon_{\rm xc}(1)\right] = \left[1-\nu\right]\left[\epsilon_{\rm xc}(1-\nu) - \epsilon_{\rm xc}(1)\right], \tag{46}$$

from which we obtain

$$\nu\epsilon'_{\rm xc}(\nu) = \nu^*\epsilon'_{\rm xc}(\nu^*) + (1-2\nu^*)\epsilon_{\rm xc}(1), \tag{47}$$

with $\nu^* \equiv 1-\nu$. This means that

$$\nu\epsilon_{\rm xc}^{\rm C}(\nu) = \nu^*\epsilon_{\rm xc}^{\rm C}(\nu^*). \tag{48}$$

We define

$$g(\nu) \equiv \nu\epsilon_{\rm xc}^{\rm C}(\nu). \tag{49}$$

Since the discontinuities in the chemical potential at fractional QHE fillings p/q is a relation for $d\left[\nu\epsilon_{\rm xc}(\nu)\right]/d\nu$, it is easier to work with $g(\nu)$ than with $\epsilon_{\rm xc}^{\rm C}(\nu)$. Then particle-hole symmetry implies that

$$\frac{dg}{d\nu} = -\frac{dg(\nu^*)}{d\nu^*}. \tag{50}$$

At fractional QHE fillings p/q, we must have

$$\frac{d}{d\nu}\,g(\nu)|_{\nu=(p/q)^+} - \frac{d}{d\nu}\,g(\nu)|_{\nu=(p/q)^-} = q(\mu_+ + \mu_-), \tag{51}$$

where μ_+ and μ_- are the quasi-particle and quasi-hole creation energies (defined to be positive), respectively. We construct $g(\nu)$ for $0 \le \nu \le 1/2$ to be piece-wise smooth, with $g(\frac{p}{q}) = 0$ for p/q a fractional QHE filling, and a discontinuity in the derivative given by Eq. (51).

We only included the cusps at $\nu = 1/3,\, 2/5$, their particle-hole conjugates, and the corresponding values at fillings inreased by unity. For $\nu < 1/3$, we make the Ansatz

$$g(\nu) = \alpha\nu q\mu_-(p/q)\left(\nu - p/q\right)\left[e^{(\nu-p/q)} - g_0\right], \tag{52}$$

with $p/q = 1/3$ and

$$\alpha = \frac{q}{p(1-g_0)} \tag{53}$$

and $g_0 = \exp(-p/q)$.

For $2/5 < \nu \leq 1/2$ we take

$$g(\nu) = \frac{5}{a}\mu_+(2/5)\left[1 - e^{-a_0(\nu-2/5)}\right], \tag{54}$$

with $a_0 = 80$.

Next, for $1/3 < \nu < 2/5$ we used a cubic interpolation

$$g(\nu) = a(\nu - 1/3)(\nu - 2/5)(\nu - \nu_3). \tag{55}$$

Fixing the slope of $g(\nu)$ at $(1/3)^+$ and $(2/5)^-$ then yields

$$a = \frac{3\mu_+(1/3)}{(1/3 - 2/5)(1/3 - \nu_3)}, \tag{56}$$

and

$$\nu_3 = \frac{5\mu_-(2/5)/3 + 6\mu_+(1/3)/5}{\mu_+(1/3) + 5\mu_-(2/5)}. \tag{57}$$

Finally, we smooth out the resulting discontinuities in $V_{\rm xc}$ over an interval 2δ about the fractional QHE fillings $\nu = p/q$. To do this, we interpolate linearly $g(\nu)$ between its values at $\nu = p/q \pm \delta$, so that $dg(\nu)/d\nu = A + B(\nu - p/q + \delta)$, where $A = g(p/q - \delta)$ and $B = \left[g(p/q + \delta) - g(p/q - \delta)\right]/(2\delta)$. Simple integration then yields $g(\nu) = A\nu + \frac{1}{2}B\nu^2 - B\nu(\frac{p}{q} - \delta) + C$, where C is an integration constant given by

$$C = g(p/q - \delta) - A(p/q - \delta) + \frac{1}{2}B(p/q - \delta)^2. \tag{58}$$

---

[1] K. v. Klitzing, G. Dorda, M. Pepper, Phys. Rev. Lett. **45**, 494 (1980); D.C. Tsui, H.L. Stormer, A.C. Gossard, Phys. Rev. Lett. **48**, 1559 (1990).

[2] See, for example, *Quantum Hall Effects*, by T. Chakraborty and P. Pietiläinen, Springer, 1995.

[3] B.I. Halperin, Phys. Rev. B **25**, 2185 (1982).

[4] C.W.J. Beenakker, Phys. Rev. Lett. **64**, 216 (1990).

[5] D.B. Chklovskii, B.I. Shklovskii, and L.I. Glazman, Phys. Rev. B **46**, 4026 (1992).

[6] N.B. Zhitenev, M. Brodsky, R.C. Ashoori, M.R. Melloch, SISSA preprint No. cond-mat/9601157.

[7] N.B. Zhitenev, R.J. Hang, K. von Klitzing, and K. Eberl, Phys. Rev. Lett. **71**, 2292 (1993); G. Ernst, N.B. Zhitenev, R.J. Hang, K. von Klitzing, and K. Eberl, Surf. Sci. **361/362**, 102 (1996).

[8] J.M. Shilton *et al.*, J. Phys.: Condens. Matter **8**, L337 (1996); A. Knäbchen and Y.B. Levinson, SISSA preprint No. cond-mat/9608074.

[9] P.L. McEuen *et al.*, Physica B **189**, 70 (1993) and Phys. Rev. B **45**, 11419 (1992); see also R.C. Ashoori *et al.*, Phys. Rev. Lett. **71**, 613 (1993) and Surf. Sci. **305**, 558 (1994); O. Klein *et al.*, Phys. Rev. Lett. **74**, 785 (1995).

[10] S.-R. Eric Yang, A.H. MacDonald, and M.D. Johnson, Phys. Rev. Lett. **73**, 3194 (1993).

[11] Kang-Hun Ahn, J.H. Oh, and K.J. Chang, Phys. Rev. B **52**, 13757 (1995).

[12] For a review, see, for example, *Field Theories of Condensed Matter Systems*, by E. Fradkin (Addison-Wesley, Redwood City, 1991).

[13] E. Goldman and S. R. Renn, SISSA preprint No. cond-mat/9606015; D.B. Chklovskii, Phys. Rev. B **51**, 9895 (1995); for general theory see L. Brey, Phys. Rev. B **50**, 11861 (1994).

[14] O. Heinonen, M.I. Lubin, M.D. Johnson, Phys. Rev. Lett. **75**, 4110 (1995).

[15] O. Heinonen, M.I. Lubin, and M.D. Johnson, Int. J. Quantum Chem.: Quantum Chem. Symp. **30**, 231 (1996).

[16] P. Hohenberg and W.Kohn, Phys. Rev. **136**, B864 (1964).

[17] M. Levy, Proc. Nat. Acad. Sci. U.S.A. **76**, 6062 (1979).

[18] L.H. Thomas, Proc. Camb. Phil. Soc. **23**, 542 (1926); E. Fermi, Z. Phys. **48**, 73 (1928).

[19] See, for example, N.H. March, in *Theory of inhomogeneous electron gas*, pp. 1-77, ed. by S. Lundqvist and N.H. March, (Plenum Press, New York and London, 1983).

[20] W.Kohn and L.J.Sham, Phys. Rev. **140**, A1133 (1965).
[21] B.I. Halperin, Helv. Phys. Acta **56**, 75 (1983).
[22] F.C. Zhang, T. Chakraborty, Phys. Rev. **B30**, 7320 (1984).
[23] U. von Barth and L. Hedin J. Phys. C, **5**, 1629 (1972).
[24] O. Gunnarsson and B.I. Lundqvist, Phys. Rev. B **13**, 4274 (1976).
[25] J.P. Perdew and A. Zunger, Phys. Rev. B **23**, 5048 (1981).
[26] For a review, see R.O. Jones and O. Gunnarsson, Rev. Mod. Phys., **61**, 689 (1989).
[27] A. Svane and O. Gunnarsson, Phys. Rev. Lett. **65**, 1148 (1990); Z. Szotek, W. Temmerman and H. Winter, Phys. Rev. B **47**, 4029 (1993).
[28] M. Levy, Phys. Rev. A **26**, 1200 (1982); M. Levy and J.P. Perdew in *Density functional methods in physics* ed. by R.M. Dreizler and J. da Providencia, Plenum (1985).
[29] E.H. Lieb, Int. J. Quantum Chem., **24**, 243 (1983).
[30] *Density Functional Theory*, by R. Dreizler and E.K.U. Gross (Springer Verlag, Berlin 1990)
[31] See, for example, G.D. Mahan, *Many-Particle Physics*, 2nd ed., p.77.
[32] The original paper of Levy (Ref. 28) dealt with open-shell atoms with degenerate orbitals; for another ensemble extension of DFT to the so-called equi-ensembles of excited states, see E.K.U Gross, L.N. de Oliveira and W. Kohn, Phys. Rev. A **37**, 2805 (1988), and Phys. Rev. A **37**, 2809 (1988).
[33] P.A. Maksym and T. Chakraborty, Phys. Rev. Lett. **65**, 108 (1990).
[34] M.Ferconi and G. Vignale, Phys. Rev. B **50**, 14722 (1994).
[35] T. Schmidt *et al.*, Phys. Rev. B **51**, 5570 (1995).
[36] V. Fock, Z. Phys. **47**, 446 (1928); C.G. Darwin, Proc. Cambridge Philos. Soc. **27**, 86 (1930); R. B. Dingle, Proc. Roy. Soc. London **A211**, 500 (1952).
[37] D. Levesque, J.J. Weiss and A.H. MacDonald, Phys. Rev. B **30**, 1056 (1984).
[38] R. Morf and B.I. Halperin, Phys. Rev. B **33**, 221 (1986); N. d'Ambrumenil and R. Morf, Phys. Rev. B **40**, 6108 (1989).
[39] A.H. MacDonald, S.R.E. Yang and M.D. Johnson, Austr. J. Phys. **46**, 345 (1993).
[40] A.H. MacDonald, S.R. Eric Yang and M.D. Johnson, Aust. J. Phys. **46**, 345 (1993).
[41] C. de C. Chamon, X.G. Wen, Phys. Rev. **B49**, 8227 (1994).
[42] G. Fano and F. Ortolani, Phys. Rev. B **37**, 8179 (1988).
[43] M. Ferconi, M. Geller and G. Vignale, Phys. Rev. B **52**, 16 357 (1995).
[44] S.E. Barrett *et al.*, Phys. Rev. Lett., **74**, 5112 (1995); A. Schmeller, J.P. Eisenstein, L.N. Pfeiffer, and K.W. West, Phys. Rev. Lett., **75**, 4290 (1995).
[45] S.L. Sondhi, A. Karlhede, S.A. Kivelson, and E.H. Rezayi, Phys. Rev. B **47**, 16419 (1993).
[46] A. Karlhede, S.A. Kivelson, K. Lejnell, and S.l. Sondhi, SISSA preprint No. cond-mat/9605095.
[47] G.L. Oliver and J.P. Perdew, Phys. Phys. Rev. A **20**, 397 (1979).
[48] P.A. Maksym, J. Phys. Cond. Matt. **1**, L6299 (1989).
[49] It is interesting to note that the spin polarizations of the ground state obtained in exact diagonalization studies (references 22 and 48) have been confirmed in recent theoretical work on spin polarizations at filling factors $\nu = \frac{p}{2n+1}$, where p and n are any positive integers, by N.F. Johnson and L. Quiroga, SISSA preprint No. cond-mat/9610224.
[50] T. Chakraborty and F.C. Zhang, Phys. Rev. B **29**, 7032 (1984); E.H. Rezay, Phys. Rev. B **43**, 5944 (1991).
[51] L.Brey, H.A. Fertig, R. Coté, A.H. MacDonald, Phys. Rev. Lett., **75**, 2562 (1995).

	Potential Energy					$\delta\epsilon_{\rm xc}(\nu)$	Ground state
ν	$\xi=1$	$\xi=\frac{1}{3}$	$\xi=0.5$	$\xi=\frac{2}{3}$	$\xi=0$		
$\frac{1}{3}$	-0.4152		-0.4120		-0.4135	0.0017	Polarized
$\frac{2}{7}$	-0.3870		-0.3868		-0.3884	-0.0014	Unpolarized
$\frac{2}{5}$	-0.4403		-0.4410		-0.4464	-0.0057	Unpolarized
$\frac{4}{13}$	-0.3975		-0.3997		-0.3970	0.0005	Partially polarized
$\frac{4}{11}$	-0.4219		-0.4278		-0.4241	-0.0022	Partially polarized
$\frac{4}{9}$	-0.4528		-0.4600		-0.4554	-0.0030	Partially polarized
$\frac{2}{3}$	-0.5232	-0.5257		-0.5291	-0.5331	-0.0099	Unpolarized
$\frac{3}{5}$	-0.5010	-0.5044		-0.5096	-0.5074	0.0064	Partially polarized

TABLE I. Potential energy (per particle) for various values of spin polarization and $\delta\epsilon_{\rm xc}(\nu)$ (Eq.(42)) for the four-electron (rows 1-6, Ref.[20]) and six-electron (rows 7 and 8, Ref.[46]) systems. The Zeeman energy is not included in the energy values. The unit of energy is $(e^2/\epsilon_0 l_B)$.

FIG. 1. Edge reconstruction of a spin-polarized quantum dot as the magnetic field strength is increased. Plotted here is the local filling factor $\nu(r)$ for a parabolic quantum dot with $\hbar\Omega = 1.6$ meV and 40 electrons. For magnetic field strengths $B < 2.5$ T the dot forms a maximum density droplet, and for $B \approx 2.8$ T, an exchange hole is formed. For stronger magnetic fields, incompressible regions form, separated by compressible strips.

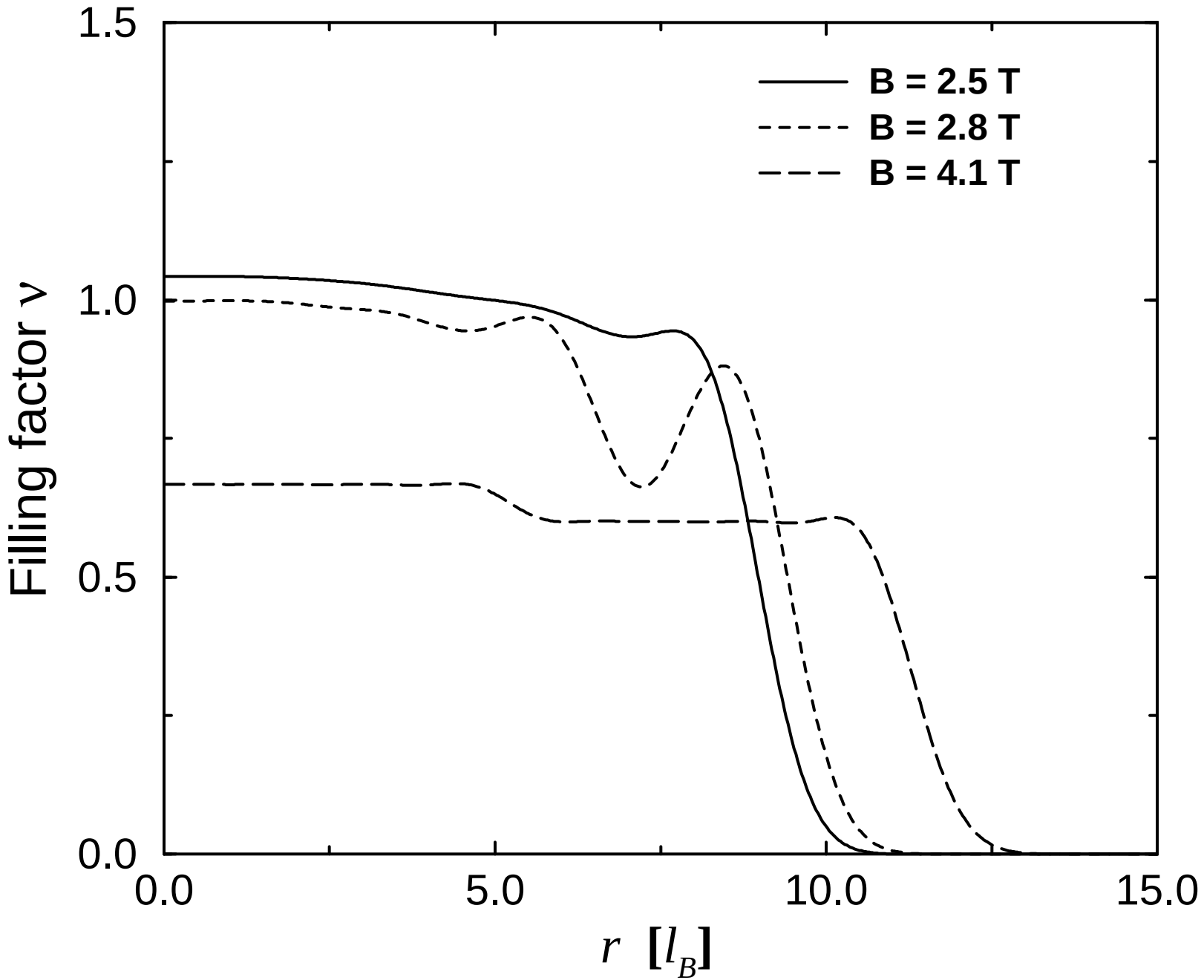
FIG. 2. Expectation value of the total angular momentum $\langle M\rangle = \sum_{mn} m f_{mn}$ as a function of the magnetic field strength B indicated by solid line for a spin-polarized six-electron droplet in a parabolic confinement using the Levesque-Weiss-MacDonald (Ref. 37) ($\diamond$) and Fano-Ortolani (Ref. 42) (+) exchange-corrleation energies. The solid shows the exact diagonalization studies result from Ref. 10.

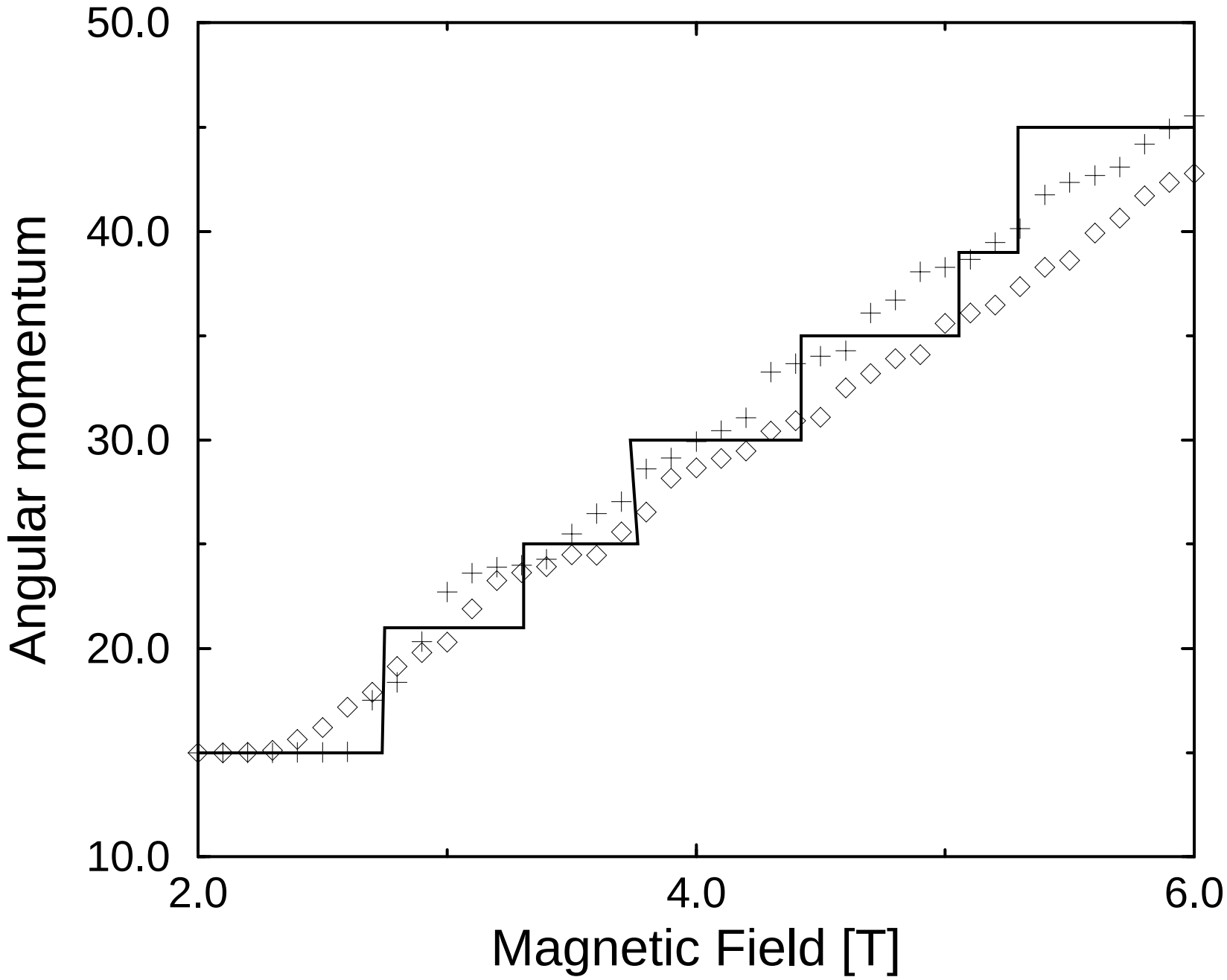
FIG. 3. Local filling factor as a function of radial coordinate for a six-particle system in a parabolic external potential with $\hbar\Omega = 2.0$ meV. Here, the Fano-Ortolani exchange-correlation energy (Ref. 42) was used. The transition to a 1/3-droplet occurs between $B = 5.3$ T and $B = 5.4$ T. The bumb in electron charge at the edge of the system is characteristic of systems with a not too soft confining potential.

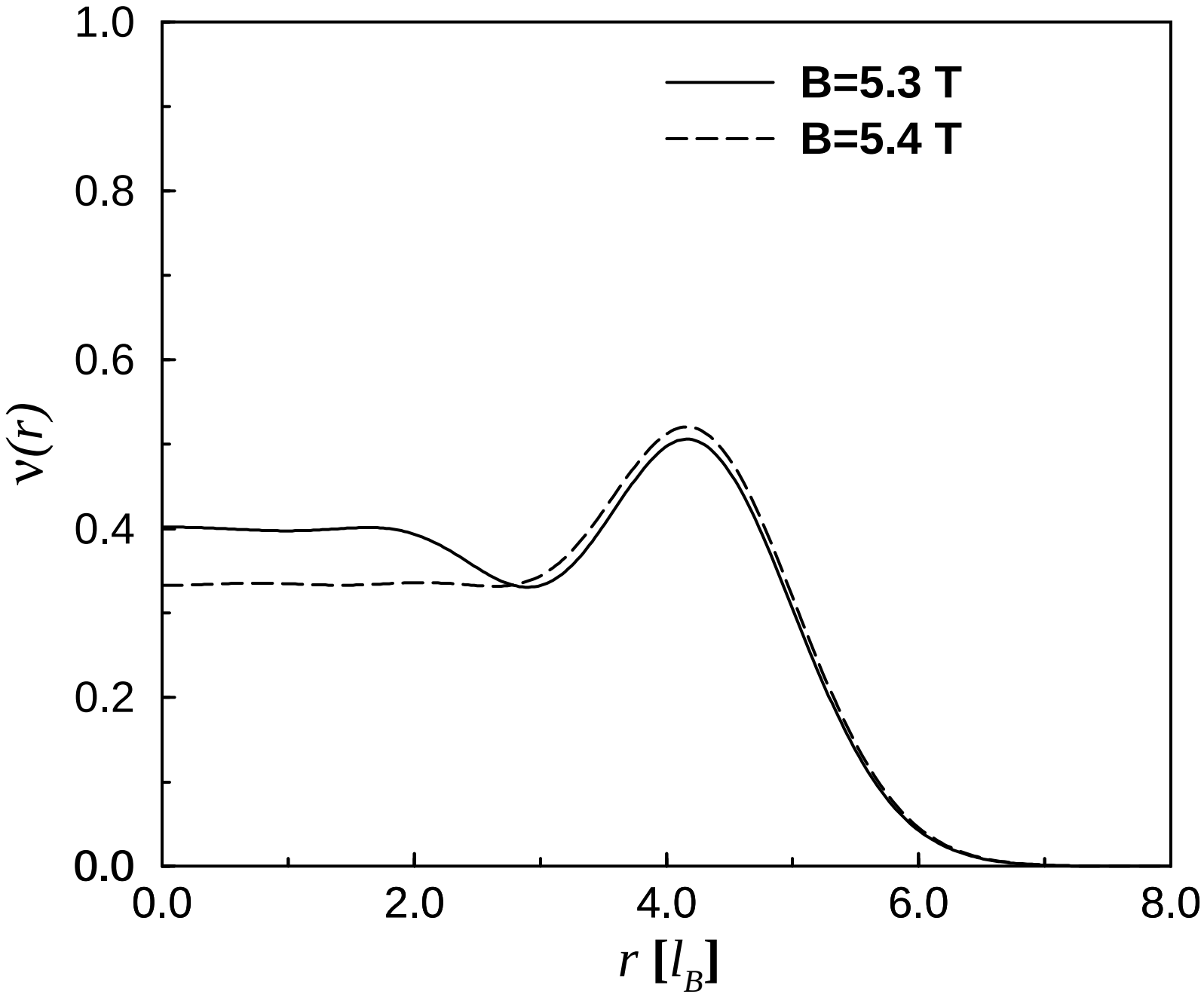
FIG. 4. The exchange-correlation potentials $V_{\mathrm{xc},\sigma}$ as a function of a filling factor ν at $\xi = 1$ and $\xi = 0$ in units of $e^2/(\epsilon_0 l_B)$. The solid line indicates $V_{\mathrm{xc},\uparrow}$ and short-dashed line corresponds to $V_{\mathrm{xc},\downarrow}$ at $\xi = 1$. According to Eqs. (45) and (41), the exchange-correlation potentials $V_{\mathrm{xc},\sigma}$ coincide at $\xi = 0$ (since $f'(0) = 0$) and are shown by the long-dashed line. The increase in V_{xc} as functions of ν at a FQHE filling factors occurs over a range of a filling factor of 0.002.

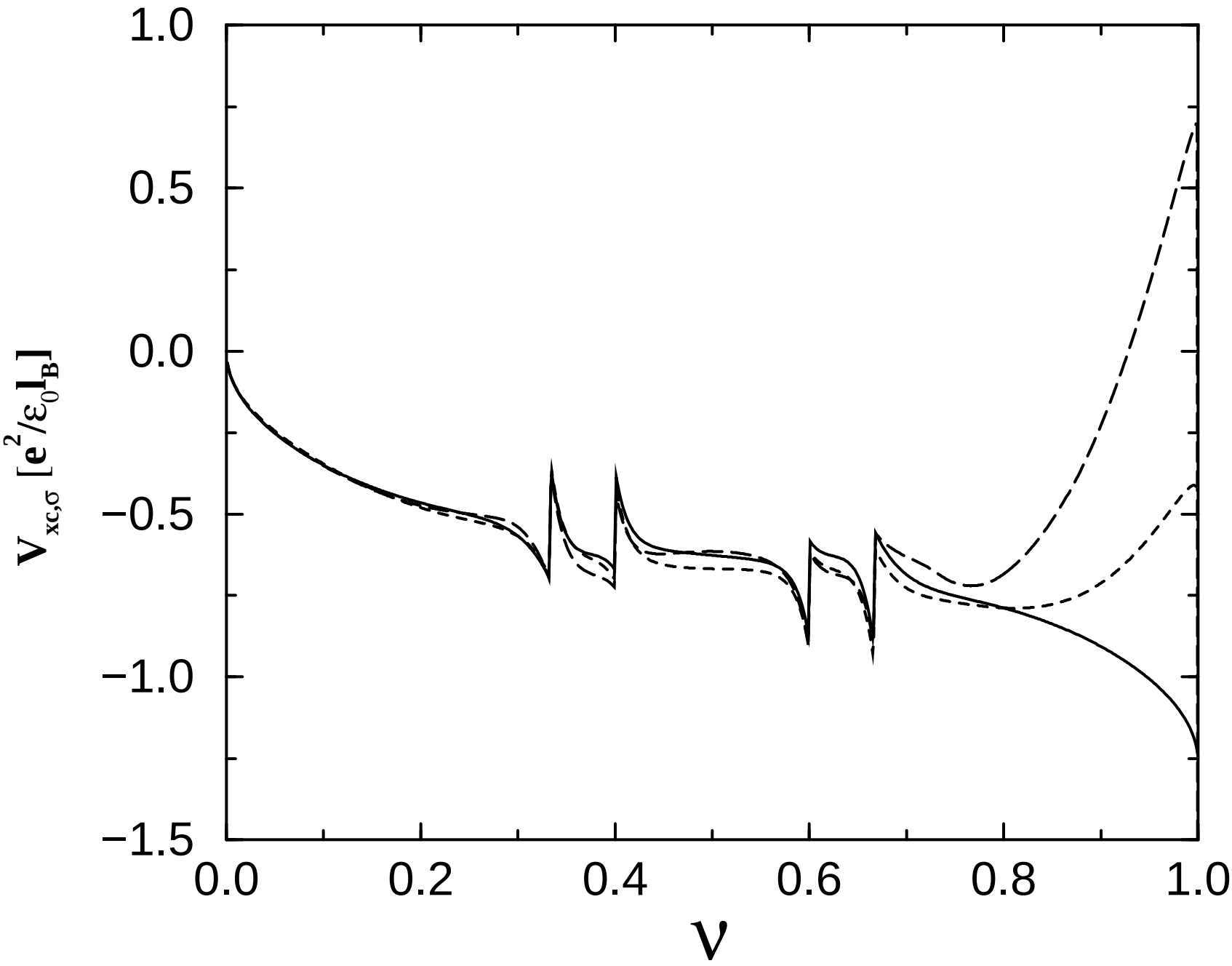
FIG. 5. Spin structured instability at the edge of a quantum dot for a Zeeman splitting $\widetilde{g} = 0.014$, magnetic field $B = 3.05$ T, and $N = 38$. The external potential is characterized by $\hbar\Omega = 1.6$ meV (so that the dimensionless strength of the confinement is $\widetilde{\gamma} = 0.063$). (a) The solid line depicts the total local filling factor $\nu(r)$ as a function of radial coordinate r, and the dashed line depicts the polarization. (b) The occupancies of the KS states $\psi_{m0,\sigma}(r)$ are plotted against orbital center coordinate $r_m = (2m)^{1/2} l_B$ with "+" for majority ($\uparrow$) spin occupancies, and "$\diamond$" for minority ($\downarrow$) spin occupancies. At the instability of the maximum density droplet for this value of $\widetilde{g}$, there is a minority-spin population at the edge of the system. (c) Eigenvalues of the two lowest Landau level KS orbitals, with + depicting eigenvalues of the majority spin orbitals, and $\diamond$ depicting the eigenvalues of the minority spin orbitals. The chemical potential is indicated by the solid line. At the edge the filling factor takes fractional values, and the KS eigenvalues are here degenerate and equal to the Fermi energy ε_F, in agreement with the general theory of Sec. II.

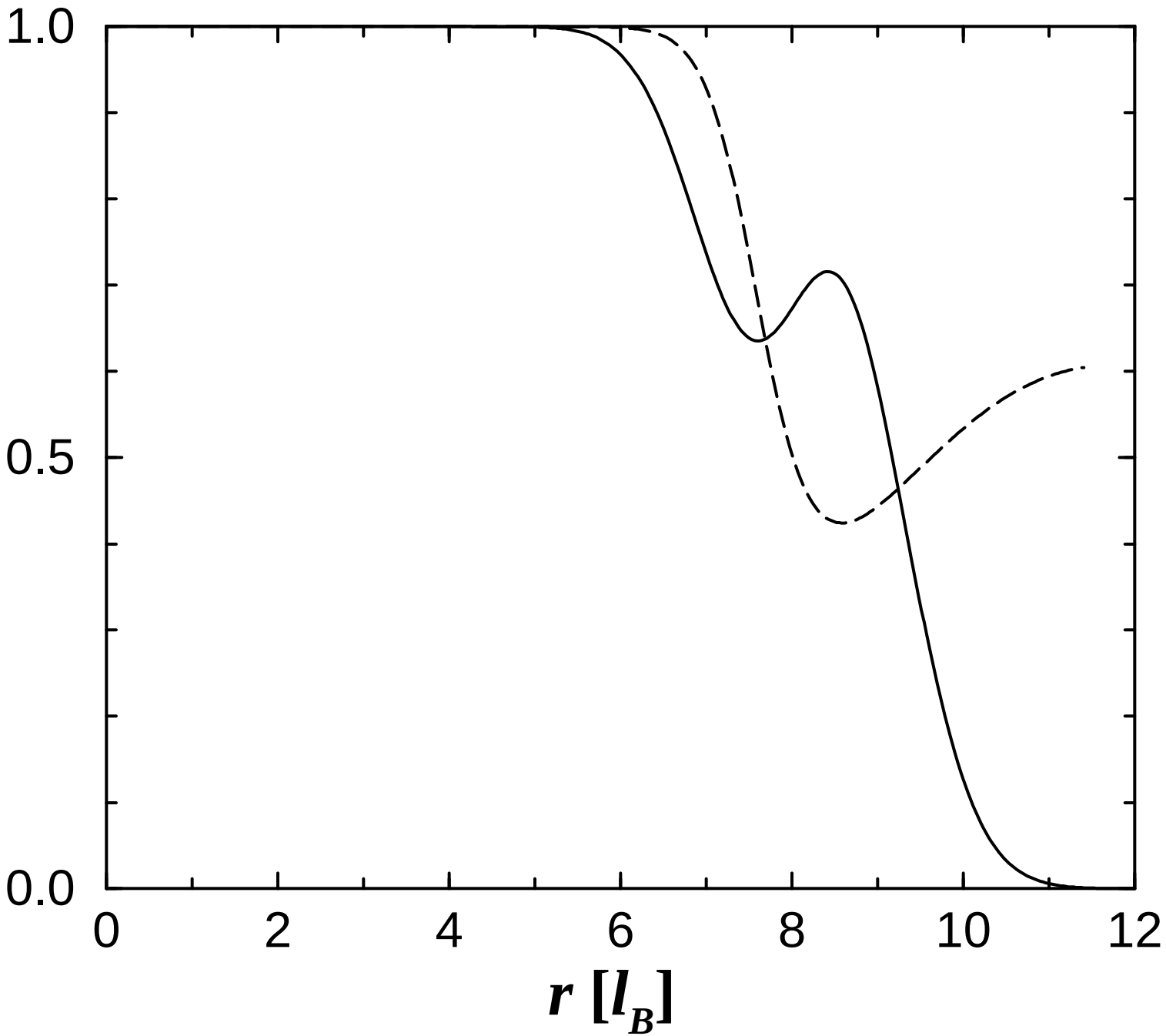
FIG. 6. Phase diagram of the edge reconstruction of a parabolic quantum dot in the $(\tilde{g}, \tilde{\gamma})$ plane for $N = 38$ electrons. Here, the confining potential has a strength given by $\hbar\Omega = 1.6$ meV. For $\widetilde{\gamma} > 0.065$, the system forms a maximum density droplet for all values of the Zeeman coupling $\widetilde{g}$. For values of the Zeeman coupling $\widetilde{g}$ larger than a critical value $\widetilde{g}_c$, the maximum density droplet undergoes an initial reconstruction to a spin-polarized exchange hole as the confinement strength $\widetilde{\gamma}$ is decreased, while for $\widetilde{g} < \widetilde{g}_c$ the maximum density droplet has a spin-structured instability with decreasing $\widetilde{\gamma}$. In these calculations, $\widetilde{g}_c \approx 0.055$.

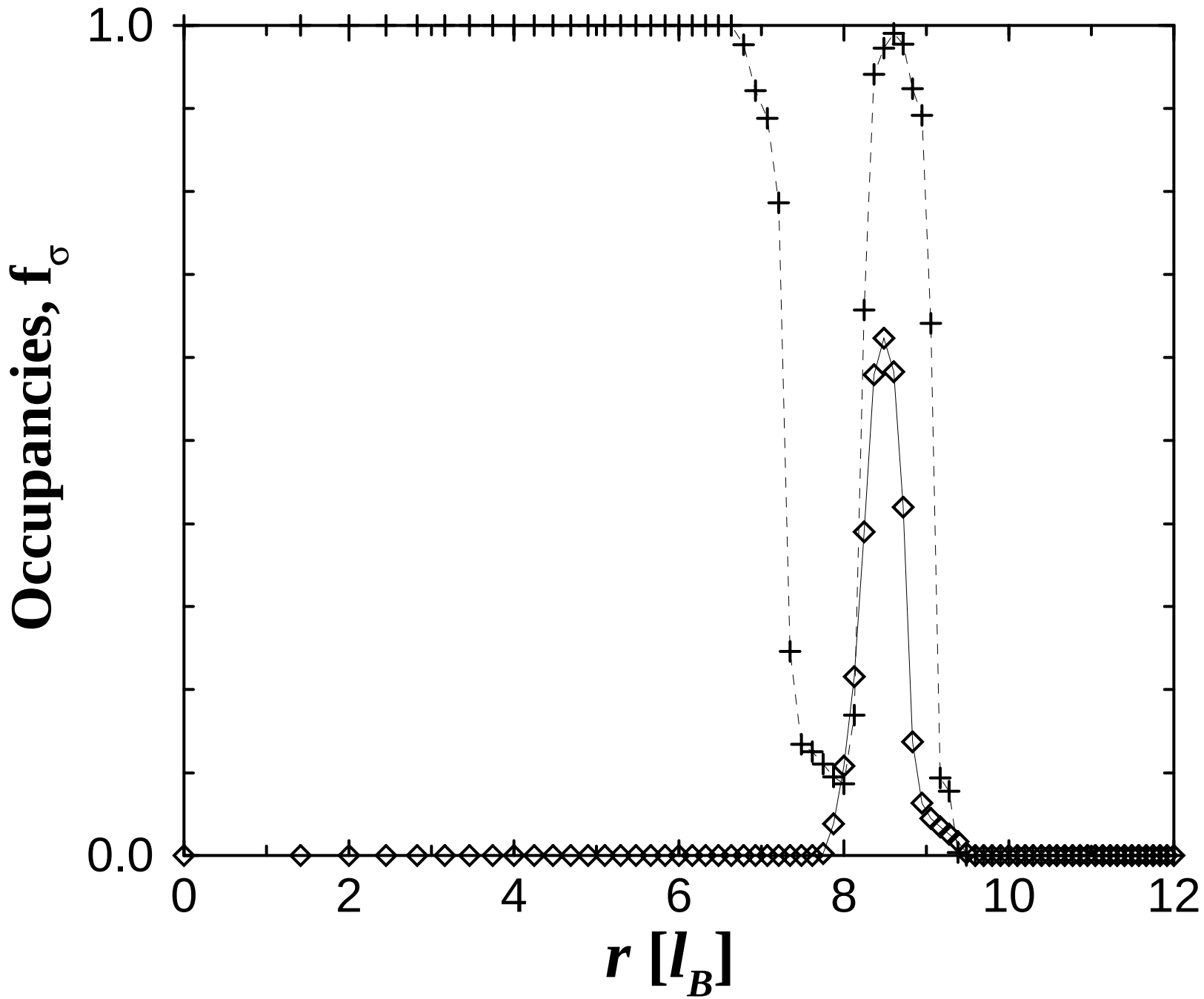

1.5
1.0
0.5
0.0
0.0
5.0
10.0
15.0
Filling factor ν
r [l_B]
B = 2.5 T
B = 2.8 T
B = 4.1 T

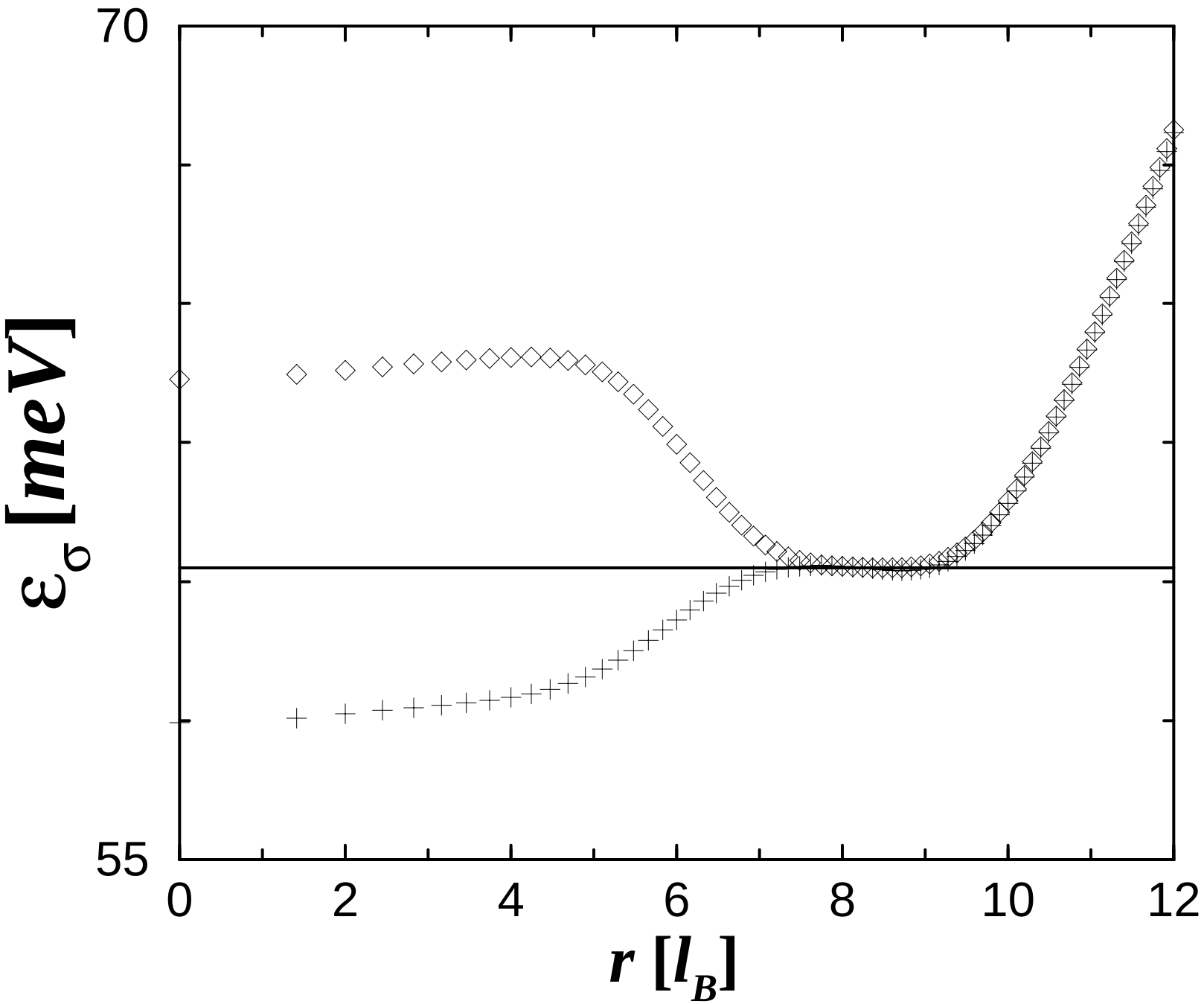

50.0
40.0
30.0
20.0
10.0
2.0
4.0
6.0
Angular momentum
Magnetic Field [T]

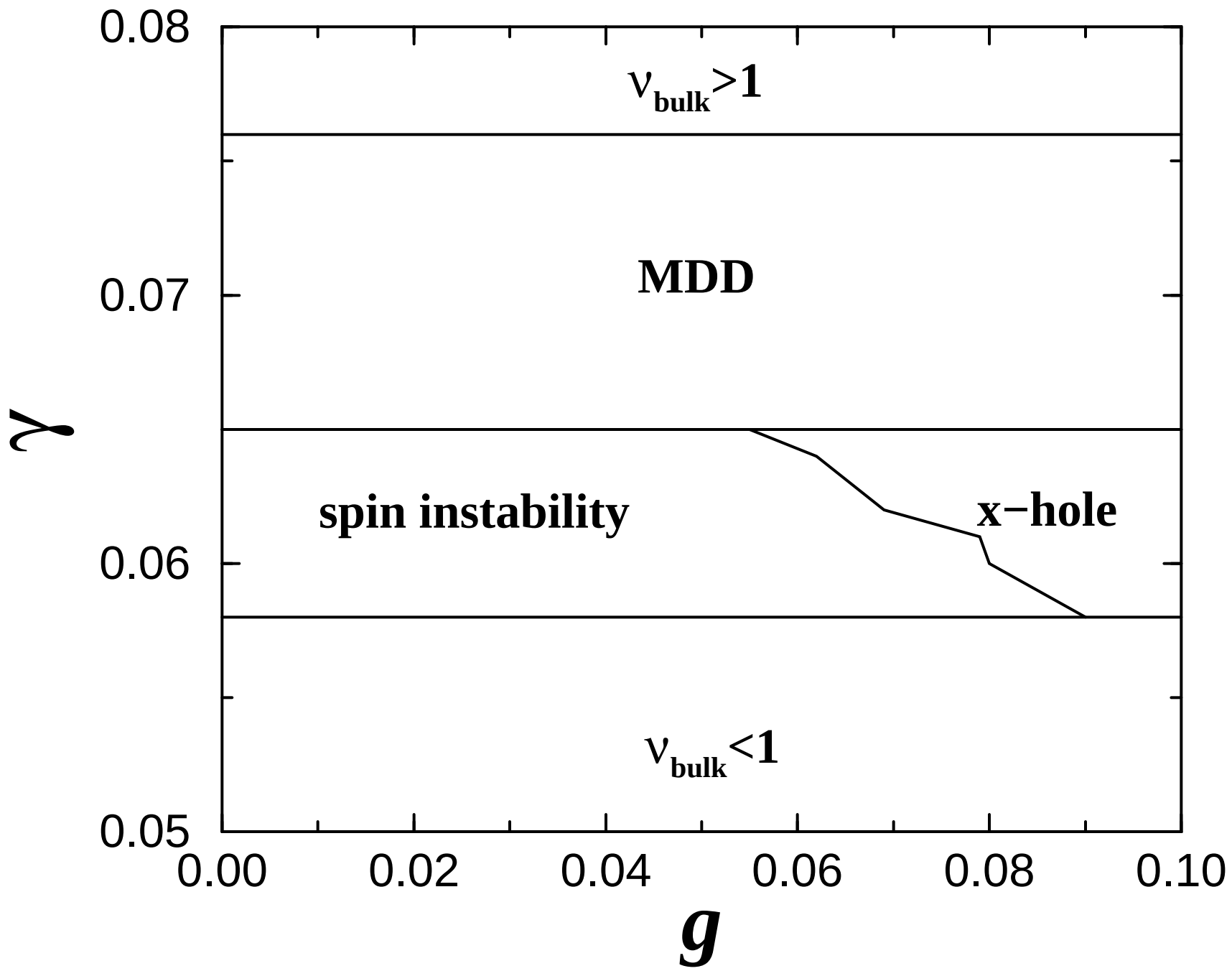

B=5.3 T
B=5.4 T
1.0
0.8
0.6
0.4
0.2
0.0
ν(r)
0.0
2.0
4.0
6.0
8.0
r [l_B]


1.0
0.5
0.0
−0.5
−1.0
−1.5
0.0
0.2
0.4
0.6
0.8
1.0
ν
$V_{xc,\sigma}$ [$e^2/\varepsilon_0 l_B$]


1.0
0.5
0.0
0
2
4
6
8
10
12
r [l_B]


1.0
0.0
0
2
4
6
8
10
12
Occupancies, f_σ
$r\ [l_B]$


70
55
0
2
4
6
8
10
12
ε_σ [meV]
r [l_B]


0.08
0.07
0.06
0.05
γ
ν_{bulk}>1
MDD
spin instability
x−hole
ν_{bulk}<1
0.00
0.02
0.04
0.06
0.08
0.10
g